EUROPEAN COMMUNITIES

CONTRACT CEE Nº FI 1W-0191-E (TT)

CHARACTERIZATION OF CLAY (BENTONITE)/CRUSHED GRANITE MIXTURES TO BUILD BARRIERS AGAINST THE MIGRATION OF RADIONUCLIDES: DIFFUSSION STUDIES AND PHYSICAL PROPERTIES.

E. Mingarro, P. Rivas, L.P. del Villar, B. de la Cruz, P. Gómez, A. Hernández, M.J. Turrero and M.V. Villar

ANNUAL PROGRESS REPORT
January 1989 - January 1990

CIEMAT

DIRECCION DE TECNOLOGIA
DIVISION DE TECNICAS GEOLOGICAS
February 1990

CIEMAT
Avenida Complutense 22
28040 MADRID (España)

INTRODUCTION

Granitic rocks are considered as one of the probable sites for the storage of high level radioactive wastes in Spain. The engineered barriers play, in this type of rocks, an essential role because they must guarantee the protection of the canister against the agressiveness of the environment, the longest possible delay of the transfer of radionuclides to the hydrogeologic environment and the isolation of the storage itself.

The materials used as barriers must meet a series of characteristics, such as: low hydraulic conductivity, high thermal conductivity, high swelling capacity, high radionuclide retention capacity and a mineralogical stability preserved for the site conditions and for a long period of time. These properties are met, in general by smectitic clays compacted at high densities.

The study of these properties in Spanish clays is the principal objective of this contract (CEC Nº FI 1W-0191-ECTT), which also considers the possibility of using illitic clays and crushed granites, in order to decrease the mineralogical disequlibrium between the barrier and the storage rock.

Once a detailed characterisation of thirty commercial Spanish clays was carried out, two of them were selected, one illitic and the other smectitic. to carry on further studies on: mechanical, hydraulic and thermal properties of the compacted blocks, radionuclide retention capacity, solution diffussivity and mineralogical stability.

1. SELECTED MATERIALS.

Samples M-15 and M-26 are the selected clay materials. Sample M-29, that was also chosen, has been rejected afterwards, due to a more detailed examination of the results obtained during the characterisation phase, reported in the 1988 annual report.

The principal characteristics of the chosen samples are the following:

Sample M-15

Table I
Mineralogical composition of the total sample

Phyllosilicates		Other minerals	
Illite	73.5%	Quartz	11.5%
Smectite	2.0%	Feld(Plag)	5.0%
Chlorite + Kaolinite	4.0%	Dolomite	2.0%
		Amorphous minerals	2.0%

TABLE II

Chemical composition of the total sample

SiO_2	- 58.60%	TiO_2	- 0.76%
Al_2O_3	- 16.48%	MnO	- <0.03%
Al_2O_3F	- 0.14%	P_2O_5	- 0.17%
Fe_2O_3	- 2.99%	SO_2	- <0.02%
Fe_2O_3F	- 1.38%	CO_2 org.	- 0.42%
FeO	- 0.67%	CO_2 inorg.	- 0.85%
CaO	- 0.82%	H_2O-	- 2.32%
MgO	- 4.06%	H_2O^+	- 4.00%
K_2O	- 5.99%		
Na_2O	- 0.22%		

OTHER PROPERTIES:

Liquid Limit	- 57% W
Specific area	- 59 m^2/g
Swelling pressure	- 0.52 MPa (ρ_d = 1.93 g/cm^3)
Dispersion	- 20.6%
Dry Density	- 1.98 g/cm^3 (123 MPa)

Sample M-26

Table III
Mineralogical composition of the total sample

Phyllosilicates		Other minerals	
Smectite	94.0%	Quartz	1.0%
		Plag	3.5%
		Calcite	0.5%
		Amorphous minerals	1.0%

TABLE IV

Chemical composition of the total sample

SiO_2	- 52.40%	TiO_2	- 0.24%
Al_2O_3	- 17.20%	MnO	- 0.03%
Al_2O_3F	- traces	P_2O_5	- 0.06%
Fe_2O_3	- 3.14%	SO_2	- 0.14%
Fe_2O_3F	- traces	CO_2 org.	- 0.22%
FeO	- 0.60%	CO_2 inorg.	- 0.33%
CaO	- 1.10%	H_2O-	- 12.84%
MgO	- 4.70%	H_2O^+	- 5.03%
K_2O	- 0.70%		
Na_2O	- 1.30%		

Sample M-26 is a montmorillonite, whose structural formula, calculated on the basis $O_{20}(OH)_4$, is the following:

$$(Si_{7.74}\ Al_{0.27})\ (Al_{2.73}(Fe^{3+})_{0.35}Ti_{0.03}(Fe^{2+})_{0.07}Mn_{0.003}Mg_{0.83})\ O_{20}\ (OH)_4\ (Ca_{0.11}\ Mg_{0.21}\ K_{0.13}\ Na_{0.37}).$$

OTHER PROPERTIES:

Liquid Limit	- 129% W
Specific area	- 449 m^2/g
CEC	- 78 meq/100g
Swelling pressure	- > 30 MPa (ρ_d = 2.0 g/cm^3)
Dispersion	- 40.6%
Dry Density	- 2.04 g/cm^3 /123 MPa)

Both clays have been used in the mixtures with crushed granite from El Berrocal, and in the manufacture of compacted blocks, on which the mechanical and hydraulical properties and the radionuclide retention capacity, described in this report, have been determined.

2. SWELLING PRESSURE AND FREE SWELLING.

The swelling capacity of the barrier material should favor the isolation of the site of the canister by sealing the interface zone among storage rock - barrier - canister and filling up the fissures in the rock.

The swelling pressure has been determined with an oedometer on compacted blocks with a standard thickness of 12 mm and diameters varying from 100 to 20 mm, depending on the expected swelling capacity and the load capacity of the oedometers.

During the time of the test, the cell of the oedometer has been kept - water saturated and the swellings have been compensated with static loads until equilibrium was reached. The height increments have been measured by a 0.01 mm deformation gauge.

$$\text{Swelling pressure} = \frac{\text{lever arm} * \text{load}}{\text{sample area}}$$

Due to the variation of the swelling capacity with the compaction density of the clay and the clay-granite mixtures, it was considered necessary to complete the data on the 1988 annual report by systematically determining the swelling pressure as a function of the density and the amount of the clay-granite mixture.

These data are interesting because they reflect the expected variations that will affect the compacted blocks from the beginning of the site construction.

Table V and Figures 1 and 2 show the results.

The results clearly show a strong dependence between the swelling pressure and the density of the compacted blocks. For the range of densities considered, the value of a dry density close to 1.8 g/cm^3 seems critical, because it is, at this point, where the gradient variation is most significant. The value of the swelling pressure increases by a factor greater than 5 when the dry density varies from $\simeq$ 1.8 and 2.0 g/cm^3.

TABLE I
Swelling pressures of clay and clay-granite mixtures

% Clay in mixture	Montmorillonite(M-26)-Granite		Illite (M-15)-Granite	
	Dry density (g/cm^3)	Swelling Pressure (Kg/cm^2)	Dry dens. (g/cm^3)	Swell. Press (Kg/cm^2)
100	1.40	6.90	1.40	0.50
100	1.57	24.00	1.60	2.50
100	1.80	63.12	1.83	12.90
100	2.13	>325.00	2.03	73.00
75	1.42	1.30	1.40	<0.40
75	1.60	8.10	1.61	0.50
75	1.81	36.10	1.80	2.90
75	2.04	250.00	2.01	18.10
50	1.38	2.90	1.40	<0.40
50	1.60	4.80	1.60	0.58
50	1.80	28.00	1.82	2.50
50	2.00	155.63	2.02	7.30
25	1.41	0.50		
25	1.58	3.40		
25	1.81	6.00		
25	2.03	60.00		

In the clay granite mixtures (not expansive) an expected decrease of the swelling pressure is produced, as a function of the amount of additives, though both parameters are not strictly proportional in the tests carried out.

On the other hand, the rate of increment density-swelling pressure increases with the amount of additive.

The montmorillonite-granite mixtures keep swelling pressures around 10 MPa for amounts of additives under 60% and within a density range of 1.85-2.0 g/cm^3.

The behaviour of illite is totally different. The maximum swelling pressure 7.3 MPa, has been obtained for 100% illite and compaction density of 2.03 g/cm^3, values which arise serious doubts on the effectiveness pf illite as a filling material. On

the other hand, the relations density-swelling pressure are similar to the ones obtained for the montmorillonite (M-26) sample.

The increase of the clay volume in the compacted block has been approximately 27% for the montmorillonite (M-26) and 12% for the illite (M-15), considering a test time ≃ 72 hours and a density ≃ 2 g/cm^3.

On Table VI and Figure 3 it is shown the relationship between swelling pressure and sample humidity for M-26.

TABLE VI
Swelling pressure vs. sample humidity (M-26)
Content of clay = 100 %

Density	Humidity (% W) Initial	Final	Swelling Press. (Kg/cm2)
1.600	10.0	38.0	24.0
1.595	16.6	39.1	33.7
1.604	20.6	38.0	43.8
1.587	26.7	48.4	44.0
1.458	35.1	49.6	16.5

From the data it can be deduced that exists a critical point for an initial humidity of the sample ranging between 20-27 % in weight for which the clays gets the highest swelling pressure.

Fig. 1 Swelling pressure clay–granite
Sample 26

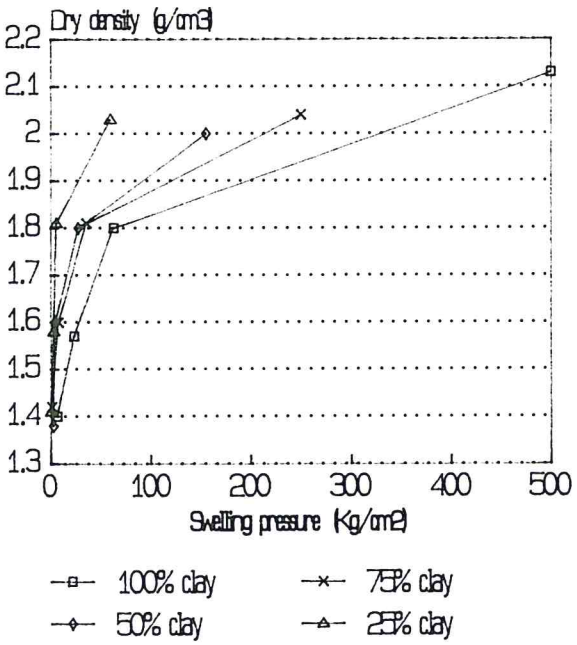

Fig. 2 Swelling pressure clay–granite
Sample 15

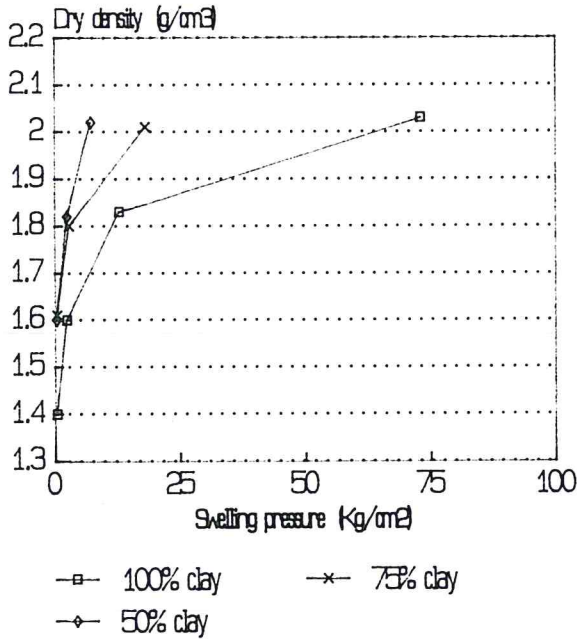

Fig. 3 Swelling pressure vs. humidity
Sample M-26 100 % Clay

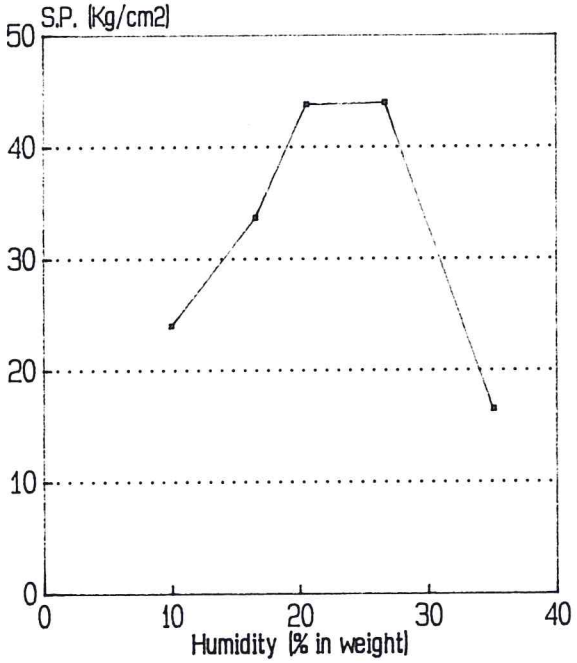

3. RESISTANCE TO SIMPLE COMPRESSION.

The object of this test is to determine the resistancce to uniaxial loads of the clay and clay-granite mixture compacted blocks, under the manufacturing conditions without confinement.

This test defines, fundamentally, the influence of the amounts of mixture and the densities obtained with constant compaction energy on the resistance of the blocks.

The resistance measurements have been carried out on blocks of initial 11.4 cm^2 cross section and 7.63 cm height, which meet the height/diameter relation ≃ 2. The unit deformation velocity of the compacted blocks has been 1%, and the load measurements have been controlled by 1000 Kg load cell and 0.2 Kg sensitivity.

The section increments, due to deformation, have been accounted for in the determination of the effective pressures on the compacted blocks.

The results are shown in Tables VII, VII and in Figures 4 through 7.

According to these results the following can be assumed:

- The behaviour upon simple compression is different in the two selected clays, montmorillonite (M-26) and illite (M-15). The resistance to compression is higher in the blocks manufactured with illite, when the amount of clay is high (100 and 75%).

TABLE VII
RESISTANCE TO SIMPLE COMPRESSION
Montmorillonite (M-26) - Granite

% Clay	Parameter	Compaction Energy (julius)		
		E = 8.6	E = 34.5	E = 138
100	Dry density (g/cm)	1.28	1.52	1.64
	Humidity (%)	21.20	20.30	18.90
	Shear tension(Kg/cm)	0.69	8.75	15.90
	Deformation (%)	2.00	2.00	2.00
75	Dry density (g/cm)	1.37	1.64	1.72
	Humidity (%)	17.20	16.80	17.60
	Shear Tension(Kg/cm)	1.48	9.20	17.75
	Deformation (%)	2.00	2.00	2.60
50	Dry density (g/cm)	1.43	1.72	1.86
	Humidity (%)	15.00	14.30	14.60
	Shear Tension(Kg/cm)	1.30	7.85	14.25
	Deformation (%)	3.00	2.63	4.53
25	Dry density (g/cm)	1.52	1.79	1.89
	Humidity (%)	12.50	11.90	12.10
	Shear Tension(Kg/cm)	0.80	3.92	6.00
	Deformation (%)	2.63	2.63	3.00

- The addition of granite improves the resistance of montmorillonite, but only for proportions around 25%. The addition of amounts greater than 50% decreases its resistance. Both effects are enhanced when the compaction energy and the density of the blocks are increased (Fig. 4).

- The resistance to compression of the illite - built blocks decreases, remarkably, for all the granite proportions used in the mixtures. This effect is also emphasized when the compaction energy increases (Fig. 5).

TABLE VIII
RESISTANCE TO SIMPLE COMPRESSION
Illite (M-15) - Granite

% Clay	Parameter	Compaction Energy (julius)		
		E = 8.6	E = 34.5	E = 138
100	Dry density (g/cm)	1.46	1.76	1.90
	Humidity (%)	13.05	13.00	13.20
	Shear tension(Kg/cm)	2.74	15.50	24.35
	Deformation (%)	1.30	2.00	3.00
75	Dry density (g/cm)	1.56	1.93	2.03
	Humidity (%)	12.20	12.30	11.80
	Shear Tension(Kg/cm)	2.63	15.70	17.80
	Deformation (%)	2.00	2.87	3.36
50	Dry density (g/cm)	1.65	1.99	2.07
	Humidity (%)	11.40	11.60	11.10
	Shear Tension(Kg/cm)	2.20	6.90	6.30
	Deformation (%)	2.00	3.33	4.80
25	Dry density (g/cm)	1.66	1.93	2.07
	Humidity (%)	10.40	10.60	10.30
	Shear Tension(Kg/cm)	0.75	2.83	3.55
	Deformation (%)	2.00	2.00	3.00

- In relation to the 100% clay blocks, the resistance - density curves tend to increase their gradient as a function of density (Fig. 6 and 7). This tendency is maintained in the blocks built with mixtures of montmorillonite-granite (Fig. 6), while an indirect relation is observed in illite - granite blocks (Fig. 7). Except for the mixture 75% montmorillonite - 25% granite, the increments of resistance with density decrease in all the cases, when the proportion of granite in the mixture grows.

- The deformation, originated during the shear time, reaches its highest value for the mixture formed by 50% granite.

TABLE IX
Resistance to simple compression vs. humidity
Montmorillonite (M-26) - granite mixtures

% Clay	Bulk density (g/cm)	Humidity (% W)	R. S. C. (Kg/cm)	Deformation (%)
100	1.59	16.7	11.1	2.0
	1.64	18.9	15.9	2.0
	1.58	20.4	19.0	2.0
	1.57	25.4	16.3	5.0
	1.48	30.7	13.2	6.0
75	1.56	12.2	2.6	2.0
	1.59	15.9	9.7	2.0
	1.59	20.4	17.8	4.0
	1.58	25.5	9.1	5.0
	1.46	29.4	5.1	6.0

TABLE X
Resistance to simple compression vs. humidity
Illite (M-15)

% Clay	Bulk density (g/cm)	Humidity (% W)	R. S. C. (Kg/cm)	Deformation (%)
100	1.62	4.64	7.70	2.0
	1.62	11.73	5.75	2.0
	1.61	12.83	4.60	1.0
	1.64	16.93	3.60	2.0
	1.98	4.81	56.50	2.0
	1.99	10.24	52.10	3.0
	1.95	13.07	37.90	3.0
	1.84	16.81	21.40	4.0

Another experience done has been the measurements of the variations of the resistance to simple compression as a function of the humidity of the sample. In the case of montmorillonite (M-26) this has been done for a given density $\simeq$ 1.6 g/cm^3 and two different mixtures clay-granite (100 and 75%). In the other hand; for illite the experience has been carried out using two different densities ($\simeq$ 1.6 and 2.0 g/cm^3) and a fixed clay content (100 %).

The results are shown in Tables IX and X and in Figures 8 and 9.

From this results we can see that:

- For the mixtures montmorillonite - granite studied; the increase in sample humidity leads to a highest value for the resistance to simple compression with a water content around ≃ 20% in weight, while higher water contents do not show an increase in this parameter (Fig. 8).

- In the other hand, for the illite, we find that increasing the water content of the sample only leads to a sharp decrease in the resistance to simple compression for both densities studied. It is also clear that the increase in sample density causes also a great increase in the resistance to simple compression, by a factor of 8 or greater (Fig. 9).

Fig. 4 Resistance to simple compression
Sample 26

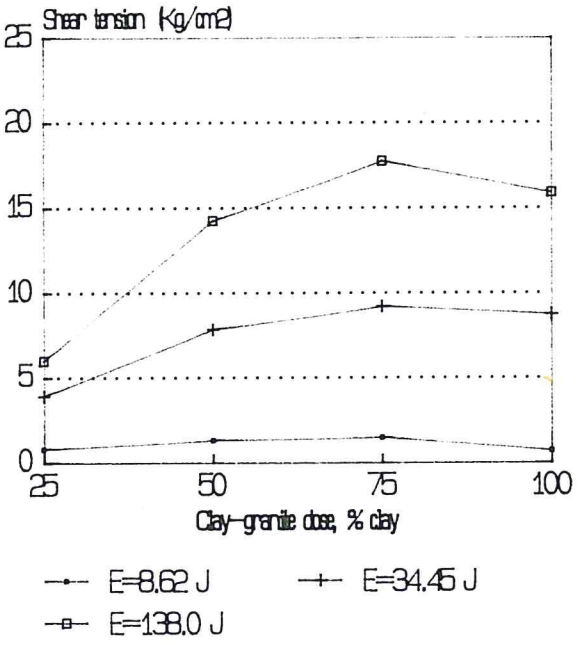

Fig. 5 Resistance to simple compression
Sample 15

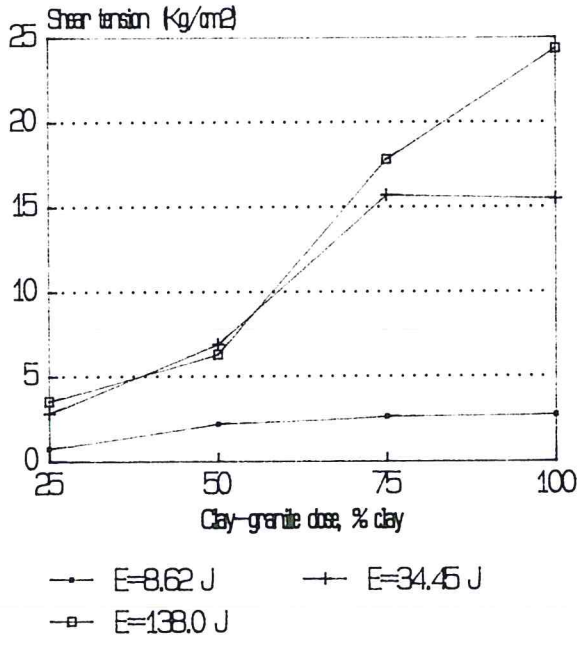

Fig. 6 Resistance to simple compression
Sample 26

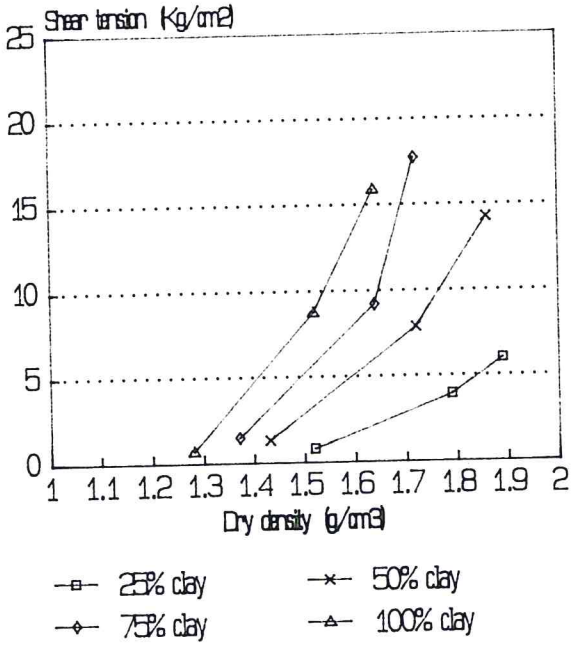

Fig. 7 Resistance to simple compression
Sample 15

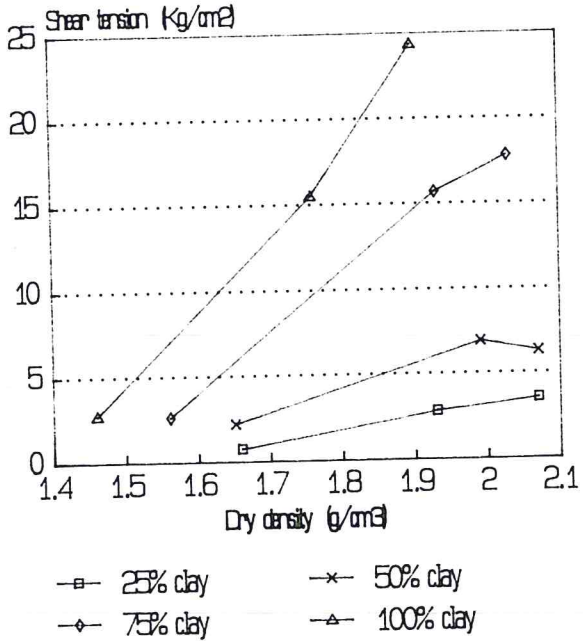

Fig. 8 Sample M-26
Resistance to simple compression
vs Humidity

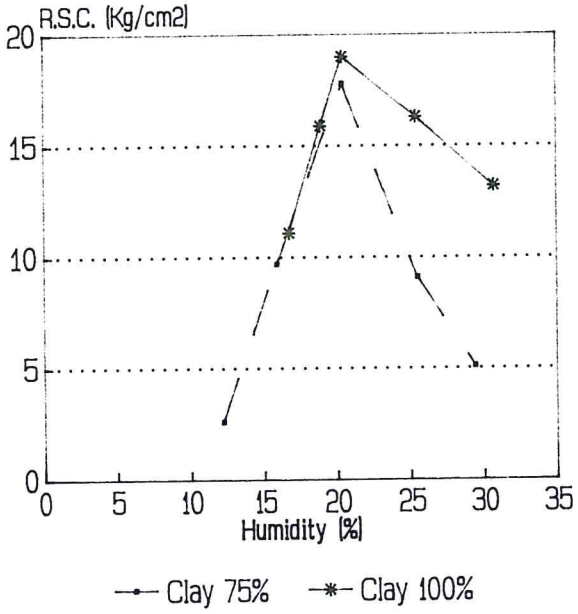

Fig. 9 Sample M-15
Resistance to simple compression
vs. humidity, for different densities.

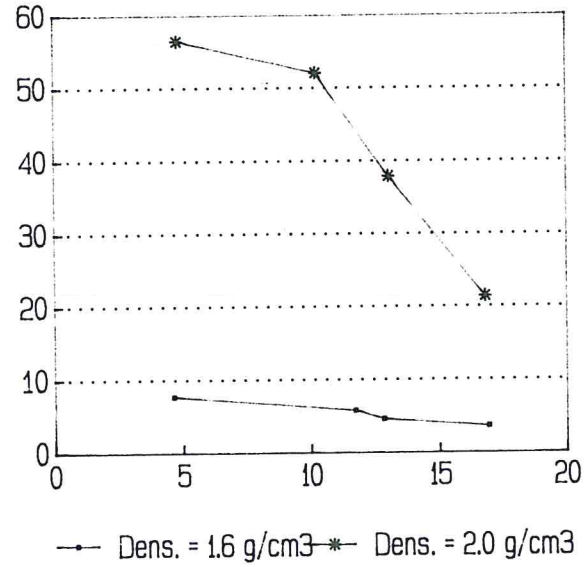

4. RESISTANCE TO SHEAR STRAIN.

The results have been obtained by triaxial tests, without previous consolidation and non-drainage shear.

The object of these tests is to obtain a valoration of the resistance parameters facing shear deformations under low confinement pressures (hydrostatic), cohesion and internal friction angle of the clay and clay - granite blocks, according to the manufacturing conditions, which theoretically, will characterize the blocks till their storage.

For a better approach to the theoretical storage conditions and an estimation of the stability of the blocks, triaxial tests have started to be carried out with hydrostatic pressures varying from 5 to 10 MPa, previous consolidation, drainage, and interstitial pressure control.

The results, shown here, correspond to the shear deformation of three compacted blocks, identically manufactured, for three different compaction energies and four proportions of mixtures (3 x 3 x 4 blocks).

As it was indicated before, the general conditions of the test were: no previous consolidation, no shear drainage and deformation speed of 1%.

The shear deformations were produced under different hydrostatic pressures: 0.5, 1.5 and 3.0 Kg/cm^2.

The results are shown in Tables XI and XII and in Figures 10 to 23, where:

σ_3 = hydrostatic or confinement pressure (Kg/cm^2)
$\sigma_1-\sigma_3$ = shift tension (Kg/cm^2)
ρ_d = dry density (g/cm^3)
w = moisture (%)
Defor = deformation (%)
c = cohesion (Kg/cm^2)
ψ = internal friction angle (°)

Based on these results, the following can be deduced:

- The hydrostatic pressure, which the compacted blocks support during the tension deformation period of time, has increased the resistance to shear deformation compared to the values obtained by simple compression. The resistance increments are related, in a certain way, to the hydrostatic pressure increments.

- The highest values for the shift tension correspond to an illitic clay, without any amount of granite.

- The addition of approximately 25% granite improves the resistance characteristics of the montmorillonite (M-26), in accordance with the simple compression tests. This effect is not detected for low compaction energies (low densities).

In the illitic clay, the shift tension decreases, in general, with the addition of granite.

Figures 10 to 15 show the variation of the shift tension, at the moment of the shear deformation, as a function of the amount of clay in the blocks.

TABLE XI
RESISTANCE TO SHEAR STRAIN
Montmorillonite (M-26) - Granite

% Clay	Parameter	Compaction energy	
		E = 8.6 julius	E = 34.5 julius
100	σ	0.50 1.50 3.00	0.50 1.50 3.00
	σ −σ	4.95 8.45 13.30	10.95 16.05 20.90
	ρ	1.39 1.40 1.41	1.55 1.55 1.56
	W(%)	10.15 9.50 8.98	9.30 9.27 9.30
	Defor	6.00 7.00 11.00	2.00 2.00 2.00
	C	0.80	1.60 - 2.00
	ψ°	39°	47° - 45°
75	σ	0.50 1.50 3.00	0.50 1.50 3.00
	σ −σ	4.50 8.20 12.70	11.20 16.80 22.00
	ρ	1.44 1.45 1.46	1.62 1.62 1.63
	W(%)	6.70 6.70 6.70	7.82 8.65 8.19
	Defor	5.00 10.00 13.00	3.00 3.00 4.00
	C	0.75	1.65 - 1.90
	ψ°	39°	47° - 43°
50	σ	0.50 1.50 3.00	0.50 1.50 3.00
	σ −σ	4.40 7.85 12.70	8.15 14.70 21.40
	ρ	1.54 1.54 1.54	1.70 1.71 1.71
	W(%)	6.50 6.80 7.00	3.04 3.02 3.03
	Defor	7.00 7.50 11.00	3.00 4.00 5.00
	C	0.67	1.00
	ψ°	38°	48° - 46°
25	σ	0.50 1.50 3.00	0.50 1.50 3.00
	σ −σ	3.30 5.90 10.10	7.50 10.80 14.80
	ρ	1.46 1.43 1.43	1.68 1.68 1.68
	W(%)	7.05 7.02 7.51	6.82 7.01 7.40
	Defor	9.00 11.00 16.00	3.00 4.00 4.00
	C	0.40	1.40
	ψ°	35°	38°

- Shift tension vs. density is represented in figures 16 to 23. As a general tendency, an increment of the shift tension - density curve gradient is observed, as well as the amount of granite in the mixtures increases.

TABLE XI (CONT.)
RESISTANCE TO SHEAR STRAIN
Montmorillonite (M-26) - Granite

% Clay	Parameter	Compaction energy E = 138 julius		
100	σ	0.50	1.50	3.00
	$\sigma - \sigma$	23.20	28.90	36.50
	ρ	1.71	1.73	1.72
	W(%)	8.00	8.20	7.90
	Defor	2.00	1.60	2.60
	C		4.40	
	$\psi°$		45°	
75	σ	0.50	1.50	3.00
	$\sigma - \sigma$	24.40	33.30	36.20
	ρ	1.78	1.79	1.77
	W(%)	6.50	6.00	6.40
	Defor	2.00	3.00	3.00
	C		3.00 - 4.50	
	$\psi°$		55° - 45°	
50	σ	0.50	1.50	3.00
	$\sigma - \sigma$	23.80	32.50	35.10
	ρ	1.84	1.85	1.88
	W(%)	9.07	8.87	8.80
	Defor	3.00	3.00	3.00
	C		3.10 - 4.50	
	$\psi°$		54° - 44°	
25	σ	0.50	1.50	3.00
	$\sigma - \sigma$	14.00	18.80	23.80
	ρ	1.86	1.86	1.85
	W(%)	6.62	6.56	6.47
	Defor	2.00	3.00	4.00
	C		2.60 - 2.40	
	$\psi°$		45° - 42°	

- Cohesion and internal friction angle decrease considerably for densities around 1.53 g/cm^3, and even for 1.68 g/cm^3 when the granite proportion is high.

TABLE XII
RESISTANCE TO SHEAR STRAIN
Illite (M-15) - Granite

% Clay	Parameter	Compaction energy	
		E = 8.6 julius	E = 34.5 julius
100	σ	0.50 1.50 3.00	0.50 1.50 3.00
	$\sigma_1 - \sigma_3$	4.50 8.25 12.50	13.90 20.50 25.80
	ρ	1.45 1.47 1.45	1.69 1.69 1.70
	W(%)	7.40 7.30 7.30	8.08 8.11 8.38
	Defor	2.00 6.00 10.00	2.00 2.00 2.00
	C	0.60 - 0.40	2.50 - 2.20
	$\psi°$	41° - 38°	48° - 44°
75	σ	0.50 1.50 3.00	0.50 1.50 3.00
	$\sigma_1 - \sigma_3$	5.20 7.80 12.50	11.40 17.50 23.50
	ρ	1.53 1.55 1.53	1.70 1.70 1.69
	W(%)	8.10 8.15 8.10	1.60 1.40 1.30
	Defor	2.00 4.00 9.00	3.00 3.00 3.00
	C	0.80	1.40
	$\psi°$	37°	50°
50	σ	0.50 1.50 3.00	0.50 1.50 3.00
	$\sigma_1 - \sigma_3$	5.95 9.90 13.90	9.30 16.30 21.75
	ρ	1.64 1.65 1.68	1.76 1.76 1.77
	W(%)	3.61 3.43 3.50	1.58 1.52 3.22
	Defor	3.00 4.00 8.00	3.00 3.00 3.00
	C	0.50 - 0.40	1.40 - 1.00
	$\psi°$	46° - 42°	50° - 46°
25	σ	0.50 1.50 3.00	0.50 1.50 3.00
	$\sigma_1 - \sigma_3$	3.20 5.40 9.05	6.25 10.05 14.50
	ρ	1.51 1.49 1.50	1.77 1.76 1.76
	W(%)	6.15 5.48 5.80	5.95 5.92 5.80
	Defor	5.00 9.00 13.00	4.00 4.50 5.00
	C	0.45	0.80 - 0.70
	$\psi°$	33°	45° - 40°

TABLE XII (CONT.)
RESISTANCE TO SHEAR STRAIN
Illite (M-15) - Granite

% Clay	Parameter	Compaction energy E = 138 julius		
100	σ	0.50	1.50	3.00
	$\sigma - \sigma$	25.00	34.00	43.60
	ρ	1.74	1.74	1.75
	W(%)	2.54	3.33	2.50
	Defor	2.00	2.00	2.00
	C		3.75	
	$\psi°$		52°	
75	σ	0.50	1.50	3.00
	$\sigma - \sigma$	21.30	29.80	38.40
	ρ	1.86	1.83	1.83
	W(%)	1.00	1.00	1.20
	Defor	2.50	2.50	3.30
	C		3.00	
	$\psi°$		51°	
50	σ	0.50	1.50	3.00
	$\sigma - \sigma$	16.40	25.30	38.80
	ρ	1.88	1.88	1.90
	W(%)	0.90	1.00	1.00
	Defor	3.00	3.00	4.00
	C		2.50 - 2.20	
	$\psi°$		50°	
25	σ	0.50	1.50	3.00
	$\sigma - \sigma$	12.10	16.95	21.90
	ρ	1.96	1.98	1.99
	W(%)	5.62	5.60	5.80
	Defor	3.00	3.00	3.00
	C		2.20 - 1.90	
	$\psi°$		45° - 42°	

Fig. 10
Sample 26 E= 8.62 J

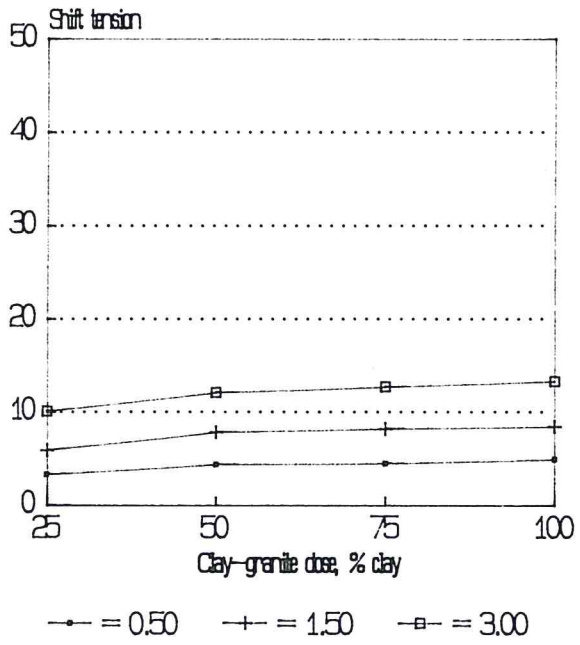

Fig. 11
Sample 26 E= 34.45 J

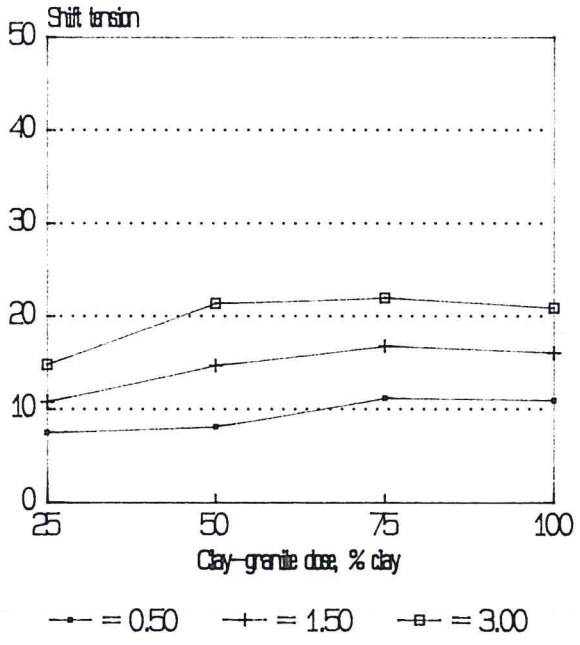

Fig. 12
Sample 26 E= 138.0 J

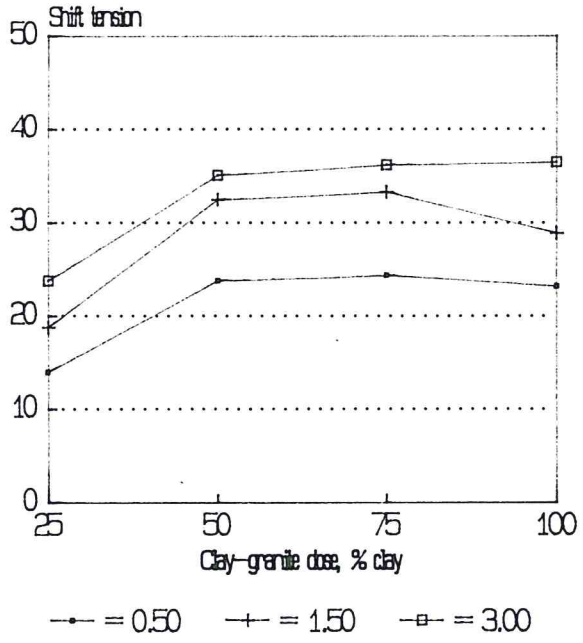

Fig. 13
Sample 15 E= 8.62 J

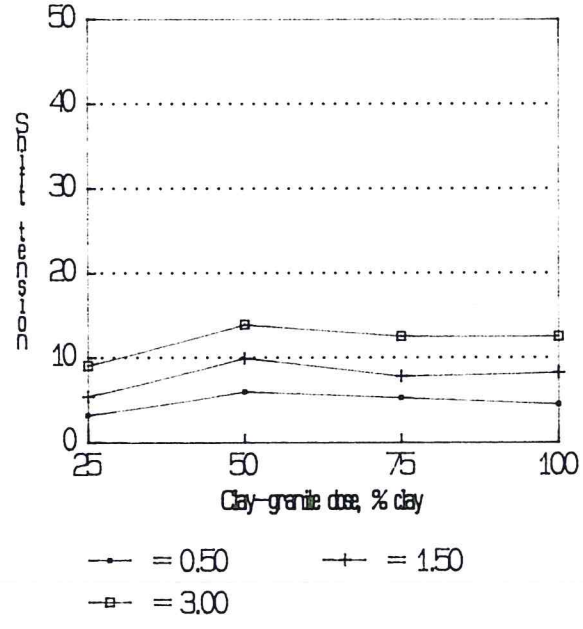

Fig. 14
Sample 15 E= 34.45 J

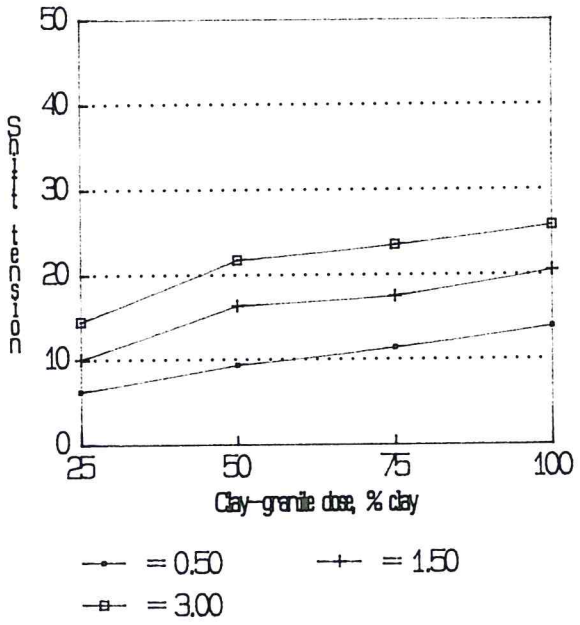

Fig. 15
Sample 15 E= 138.0 J

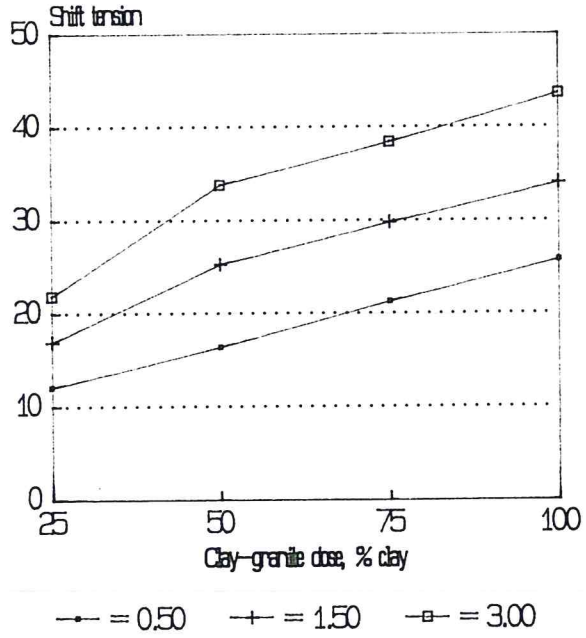

Fig. 16
Sample 26 100% clay

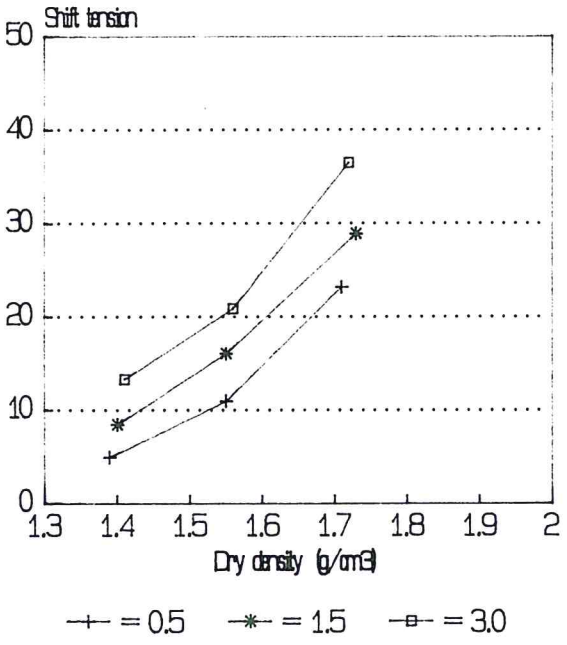

Fig. 17
Sample 26 75% clay

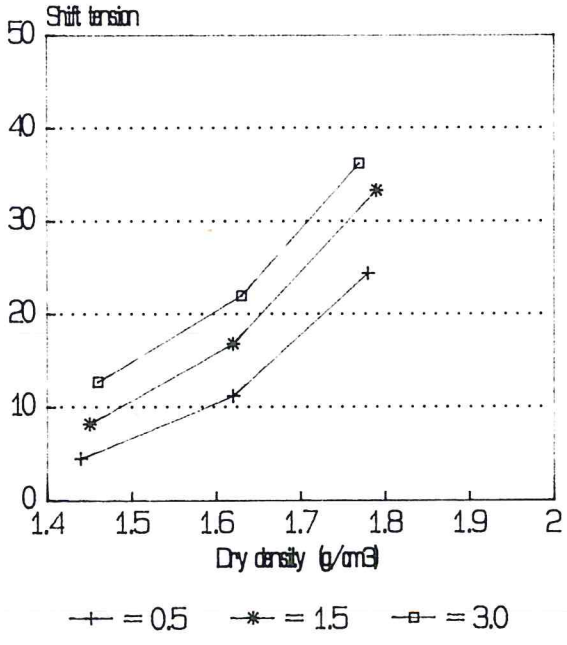

Fig. 18
Sample 26 50% clay

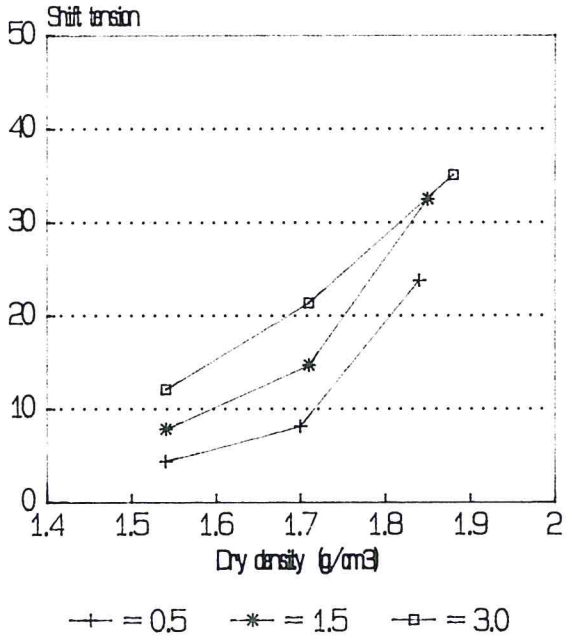

Fig. 19
Sample 26 25% clay

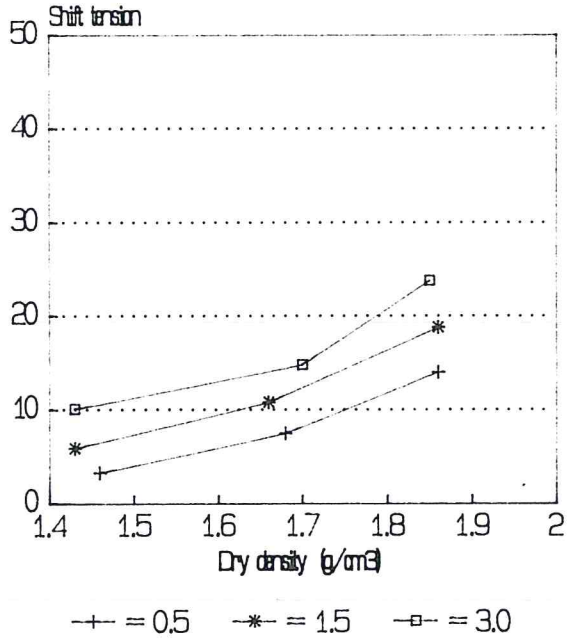

Fig. 20
Sample 15 100% clay

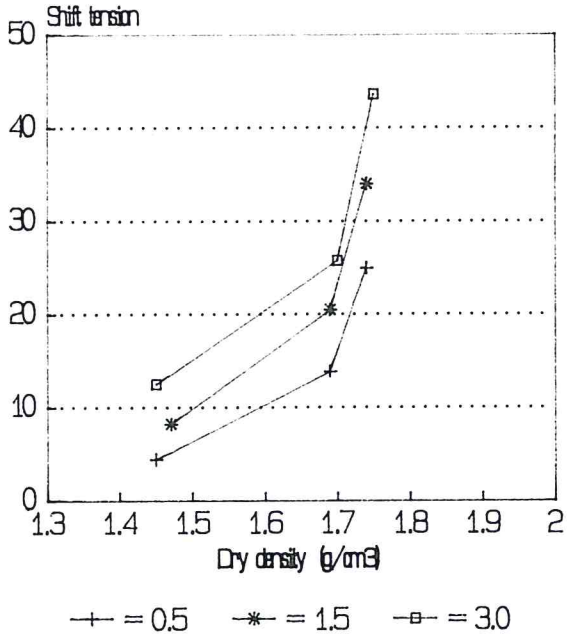

Fig. 21
Sample 15 75% clay

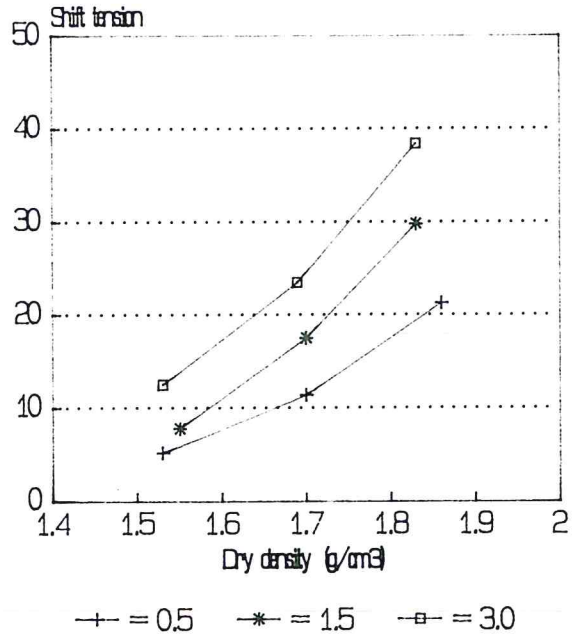

Fig. 22
Sample 15 50% clay

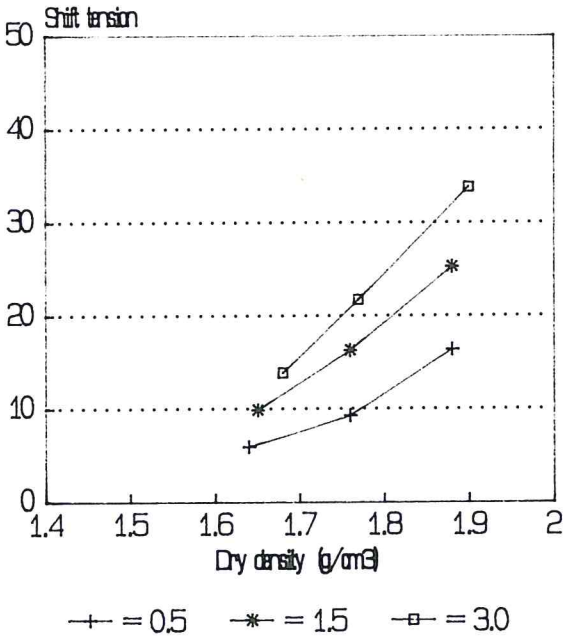

Fig. 23
Sample 15 25% clay

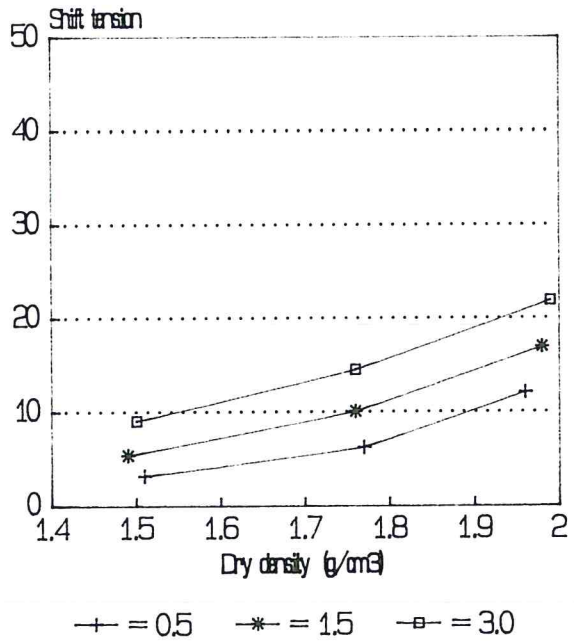

5. HYDRAULIC CONDUCTIVITY.

The hydraulic conductivity of the enginering barrier is one of the basic parameters to be taken into account, and its valuemust satisfy the requisite that the maximum speed of mass transfer through the barrier is regulated by diffussion.

The permeability coefficient has been determined on clay and clay - granite blocks, compacted at different energies and densities.

The tests have been carried out under conditions as close as possible to the expected permeability and swelling pressure values, according to the type of clay and the compaction density. For moderately low permeabilities and low swelling pressures (low density illitic and montmorillonitic blocks), triaxial cells have been used, and the blocks have been subjected to hydrostatic pressure of 7.5 Kg/cm^2 and an injection pressure of 6 Kg/cm^2 with a gradient of 1000.

For the montmorillonitic blocks (high swelling pressure and low permeability) Rowe-Barden cells are being used. In these cells the lateral swelling of the block is hindered by the sample holder ring (body of the cell) and the possible height increment can be controlled. In this system, vertical confinement, injection pressures of 11 Kg/cm^2 and a gradient of 5000 are being used.

At this moment we have started to make measurements with a new pressure equipment of 30 Tons of capacity, which also offers the possibility to carry out measurements up to 200°C.

With this new equipment for measuring hydraulic conductivity it has been possible to check out that the

previously measured values (Semestral Progress Report January - June 1989) were one or two orders of magnitude higher than the real ones, due to the modification of the dimensions of the compacted blocks during the test. The new cells, built in steel, do not allow the previously indicated modification in the blocks dimensions.

The corrected values for the hydraulic conductivity are represented in Table XIII and Figures 24 and 25.

TABLE II
HYDRAULIC CONDUCTIVITY COEFFICIENT

% Clay	Illite (M-15) - Granite		Montmorillonite (M-26) - Granite	
	Dry density (g/cm^3)	K (m/s)	Dry density (g/cm^3)	K (m/s)
100	1.40	6.4 E-10	1.40	1.3 E-12
	1.60	1.1 E-10	1.60	7.7 E-13
	1.80	3.1 E-11	1.80	3.3 E-13
	2.00	2.5 E-12	2.00	8.1 E-14
75	1.43	9.5 E-09	1.46	8.3 E-12
	1.62	3.0 E-09	1.63	5.9 E-12
	1.80	7.1 E-10	1.83	9.0 E-13
	2.00	1.8 E-10	2.00	1.3 E-13
50	1.63	2.0 E-07	1.40	1.4 E-09
	1.83	3.8 E-08	1.60	5.4 E-10
	2.03	1.5 E-08	1.80	6.3 E-11
			2.00	3.4 E-11
25	1.62	8.9 E-07	1.41	3.5 E-08
	1.80	3.6 E-07	1.65	1.4 E-08
	2.02	1.1 E-07	1.80	9.5 E-09
			2.00	4.4 E-09

The minimum value of the permeability coefficient for the illitic clay, 2.8×10^{-10} m/s, is an important handicap for its use as a barrier material, due to the decrease in density

expected under repository conditions as a consequence of the water saturation and swelling of the clay.

The addition of granite produces an important increase of the hydraulic conductivity in the compacted blocks, that together with the "in situ" expected density descent would only allow the addition of a 25% of granite in the case of the montmorillonite (M-26). For this proportion of additive the hydraulic conductivity is still of 10^{-12} m/s for densities lower than 1.6 g/cm^3.

The permeabilities measured in the montmorillonitic blocks are 1 and 2 orders of magnitude lower than the ones obtained for the illitic blocks. Permeabilities around 10^{-12} m/s or lower are expected for the montmorillonitic blocks with addition of granite up to 25%.

Fig. 24 Sample M-15
Permeability vs. Dry Density for
different clay-granite mixtures

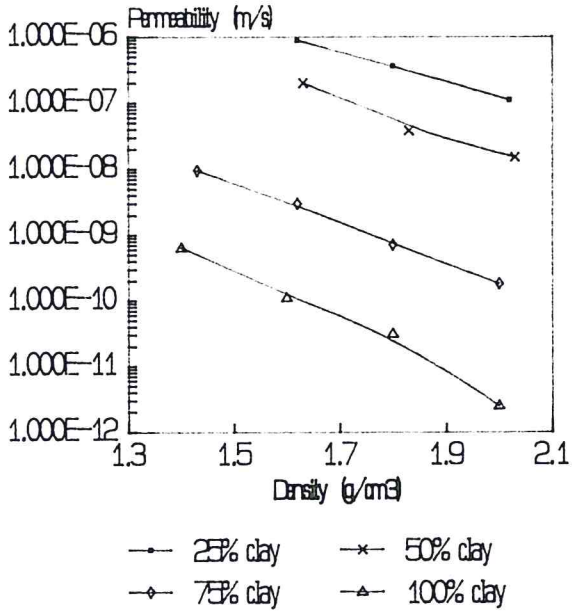

Fig. 25 Sample M-26
Permeability vs. Dry density for
different clay-granite mixtures

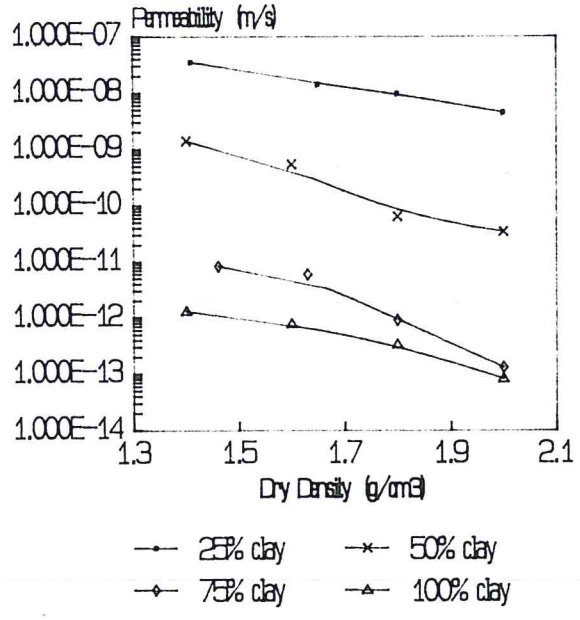

6. CONSOLIDATION ESSAYS.

The materials that form the engineered barrier will be subjected "in situ" to loads derived from the hydrostatic pressure, the weight of the clay column and the weight of the canister. Therefore it is considered of interest to know the parameters that define the behaviour of the soil in this situation.

When a material, with small particle size, is subjected to an increment in the compression efforts due to any load, the structure of the soil experiments a deformation. This elastic - plastic deformation gives as a result a reduction in the ratio of voids due to the displacement of fluids from the pores. Given the low permeability of these materials, this deformation is a slow process or time-dependent, denominated consolidation.

The determinations have been carried out with the methodology of the oedometric essay: The block of compacted clay is confined by a metalic ring in its cylilindrical contour and by porous disks on both ends, allowing the one-dimension sorption and drainage of water. The consolidation is obtained with the periodic application of increments of the load. The time interval for the application of loads has been conditioned by the definition of the secondary consolidation in each increment. At the end of the loading process the essay it is completed unloading in a staggered fashion. During all the load - unload cycle the doformations suffered by the compacted block have been registered.

The essay has been carried out with the two selected clays M-15 (Illite) and M-26 (Montmorillonite) and with the mixtures, at 75% of clay, of each one of them with molten granite. The

dimensions of the compacted blocks have varied between 20.3 and 70.7 mm in diameter and between 12 and 20 mm in height. The dry density has been 1.6 g/cm^3 and it was selected as a function of the expected density, after the "in situ" saturation and volume increment.

The results are shown in Figures 26 to 39. Figures 26, 31, 34 and 37 correspond to the oedometric curves of the variation in the pore index as a function of the pressure increments for the four samples tested. The rest of the Figures represent the consolidation curves, deformation vs. time, for the different load increments that have been used in the compacted blocks.

The consolidation characteristics of the samples tested have been expressed by the following parameters:

Compression Index: $$C_c = \frac{\Delta e}{\log(p_o+\Delta p)-\log p_o}$$

Decompression Index: $$C_s = \frac{\Delta e}{\log p_2 - \log p_1}$$

Compressibility coefficient: $$a_v = \frac{\Delta e}{\Delta p} L^2 F^{-1}$$

Volumetric compressibility coefficient: $$m_v = \frac{a_v}{1+e_o} L^2 F^{-1}$$

Consolidation coefficient: $$C_v = \frac{T_{50} H^2}{t_{50}} L^2 t^{-1}$$

The values of the oedometric parameters are expressed in Table XIV. The ratio C_c/C_s is always >1; that shows the elastic - plastic behaviour of these materials. During the unloading process, the pore index recovery in the illite is sensibly lower (C_c/C_s >3) than in montmorillonite (Cc/Cs $\geq$ 1).

In Table XV are expressed the values of the Consolidation Coefficient, C_v, for the different loading stages that have been used with each one of the samples tested. While the index of compressibility is related with the degree of settling that will take place in the sample as a function of the loads supported; the consolidation coefficient is indicative of the time in which a certain amount of consolidation will occur.

TABLE XIV
OEDOMETRIC PARAMETERS

Sample	C_c	C_s	a_v (cm^2/g)	m_v (cm^2/g)
M-15 100% Clay	0.23	0.06	8.15 E-6	4.65 E-6
M-15 75% Clay	0.05	0.006	4.40 E-6	2.60 E-6
M-26 100% Clay	0.23	0.17	1.10 E-6	7.20 E-7
M-26 75% Clay	0.21	0.18	2.70 E-6	1.80 E-6

The consolidation coefficient decreases as the process goes on and it is related to the speed of the interstitial water movement, that is a function of the permeability coefficient ($C_v = K/m_v\gamma_w$). The calculated values of K (cm/s) are also expressed in Table XV. These values decrease as the consolidation process progresses and agree with the measurements done with the

permeability cells, in the illite K varies between 10^{-9} and 10^{-10} cm/s and in montmorillonite between 10-10 and 10^{-12} depending on the degree of consolidation achieved.

TABLE XV
CONSOLIDATION AND PERMEABILITY COEFFICIENTS
FOR THE DIFFERENT LOADING STAGES

Load (Kg/cm^2)	M-15 (100% Clay)		M-15 (75% Clay)	
	C_v (cm^2/s)	K (cm/s)	C_v (cm^2/s)	K (cm/s)
1.5-3	6.4 E-4	2.9 E-09	2.5 E-4	6.5 E-10
3-6	6.0 E-4	2.8 E-09	2.5 E-4	6.5 E-10
6-10	5.3 E-4	2.5 E-09	1.9 E-4	4.9 E-10
10-15			1.7 E-4	4.3 E-10
10-20	1.3 E-3	5.9 E-09		
20-30	5.3 E-4	2.5 E-09		
20-40				
30-40	5.4 E-5	2.5 E-10		
40-60	1.1 E-4	5.3 E-10		
40-70				
70-100				
100-150				
150-200				

The consolidation of illite (ρ_d = 1.6 g/cm^3) starts for very small load values, 1.5-3 Kg/cm^2, while the montmorillonite (ρ_d = 1.6 g/cm^3) does not begin to consolidate until the stages of 10-20 Kg/cm^2 in the mixture of 75% montmorillonite-25% granite and 20-40 Kg/cm^2 for the montmorillonite without granite.

TABLE III
CONSOLIDATION AND PERMEABILITY COEFFICIENTS
FOR THE DIFFERENT LOADING STAGES

Load (Kg/cm^2)	M-26 (100% Clay)		M-26 (75% Clay)	
	C_v (cm^2/s)	K (cm/s)	C_v (cm^2/s)	K (cm/s)
1.5-3				
3-6				
6-10				
10-15				
10-20			2.3 E-4	4.1 E-10
20-30				
20-40	3.3 E-4	2.3 E-10	7.9 E-5	1.4 E-10
30-40				
40-60				
40-70	1.5 E-5	1.1 E-11	4.6 E-5	8.3 E-11
70-100	8.1 E-6	2.2 E-12	2.0 E-5	3.7 E-11
100-150	4.7 E-6	3.4 E-12		
150-200	5.1 E-6	3.6 E-12		

FIG. 26

M - 15 , Clay 100 %

OEDOMETRIC CURVE

Initial dry density: 1,60 Initial moisture: 3,7 Specific weight of the particles 2,816

Initial pore index: 0,820 Final moisture: 20,1 Sample diameter (cm): 50,47

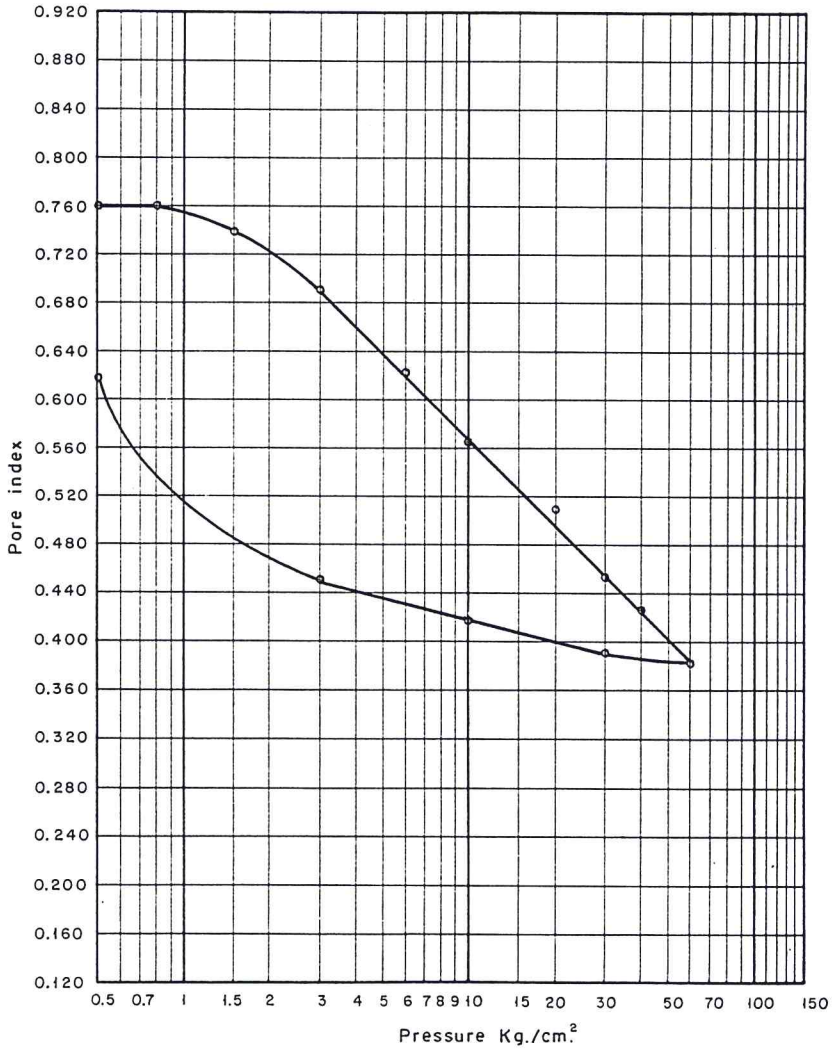

FIG. 27

M - 15 , Clay 100 %, ρ_d = 1.60 g cm^{-3}

CONSOLIDATION CURVES

Initial measure of the quarter with null load: 500 Edometer height: 20 mm

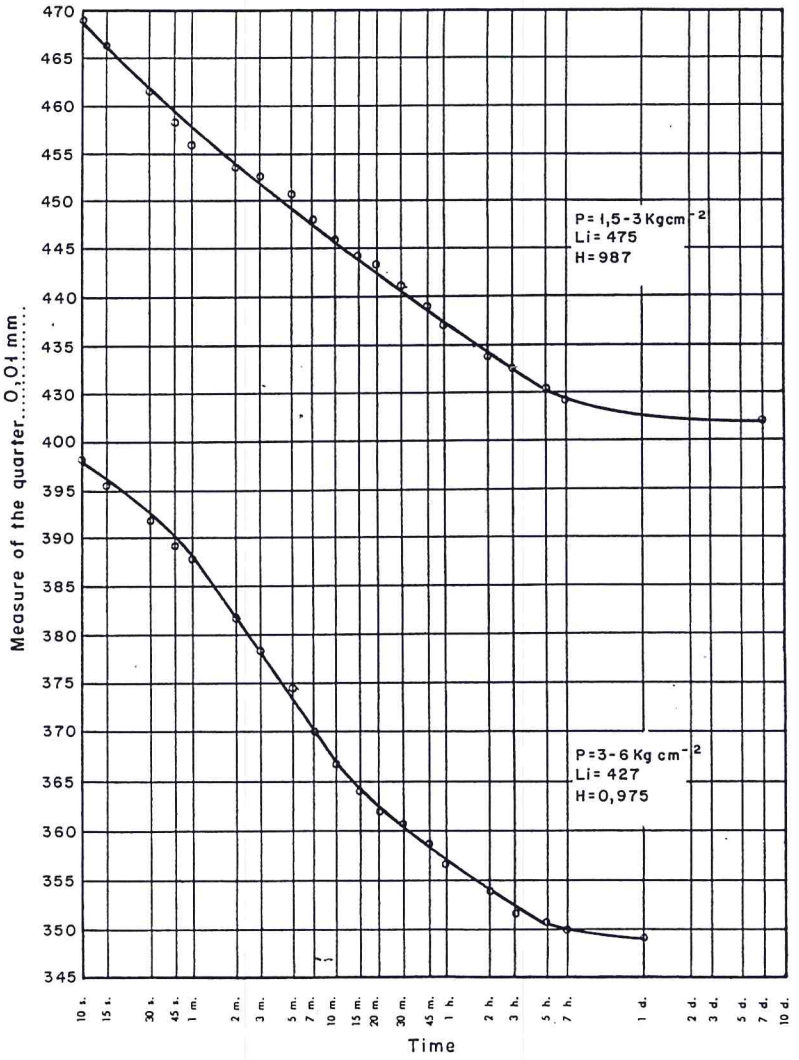

FIG. 28

M - 15 , Clay 100 %, ρ_d = 1.60 g cm^{-3}

CONSOLIDATION CURVES

Initial measure of the quarter with null load: 500 Edometer height: 20 mm

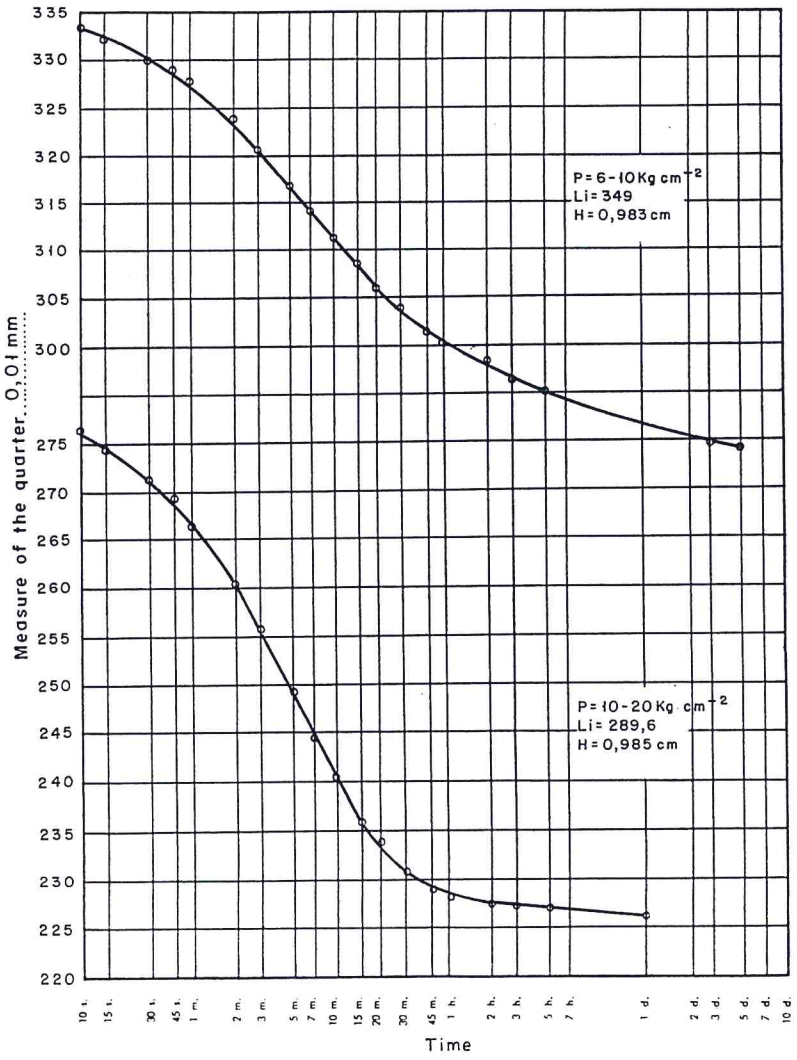

FIG. 29

M - 15 , Clay 100 %, ρ_d = 1,60 g cm^{-3}

CONSOLIDATION CURVES

Initial measure of the quarter with null load: 500 Edometer height: 20 mm

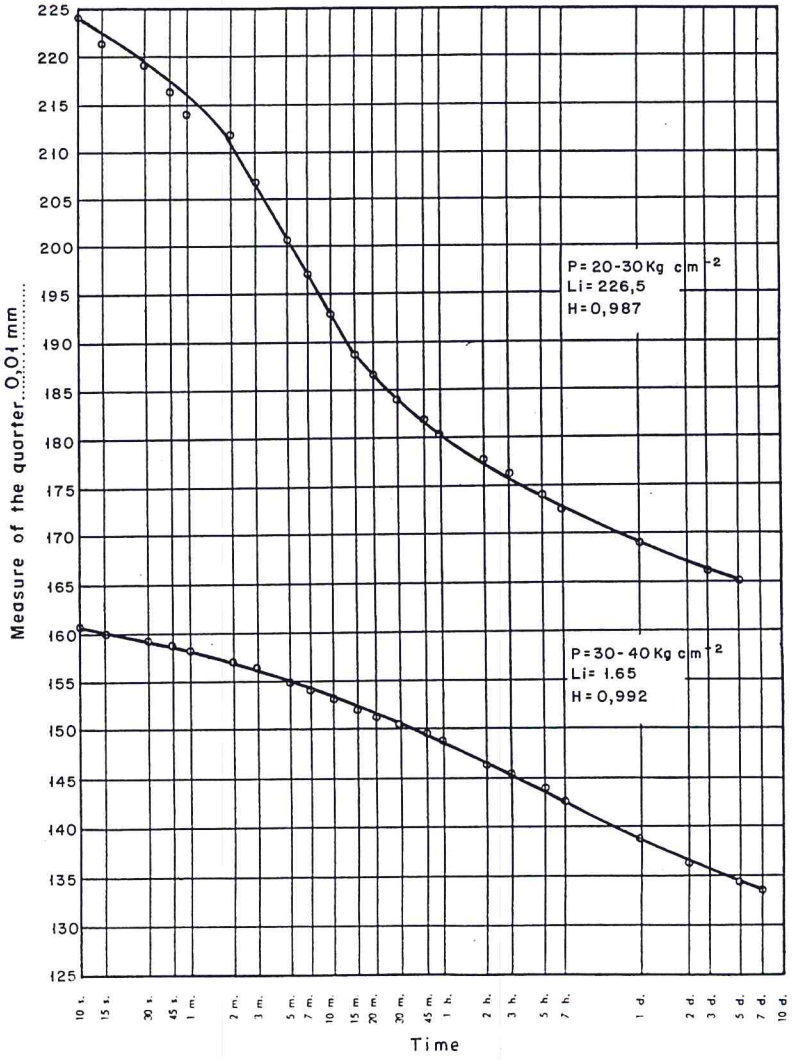

FIG. 30

M - 15 , Clay 100 %, ρd = 1.60 g cm^{-3}

CONSOLIDATION CURVES

Initial measure of the quarter with null load: 500 Edometer height: 20 mm

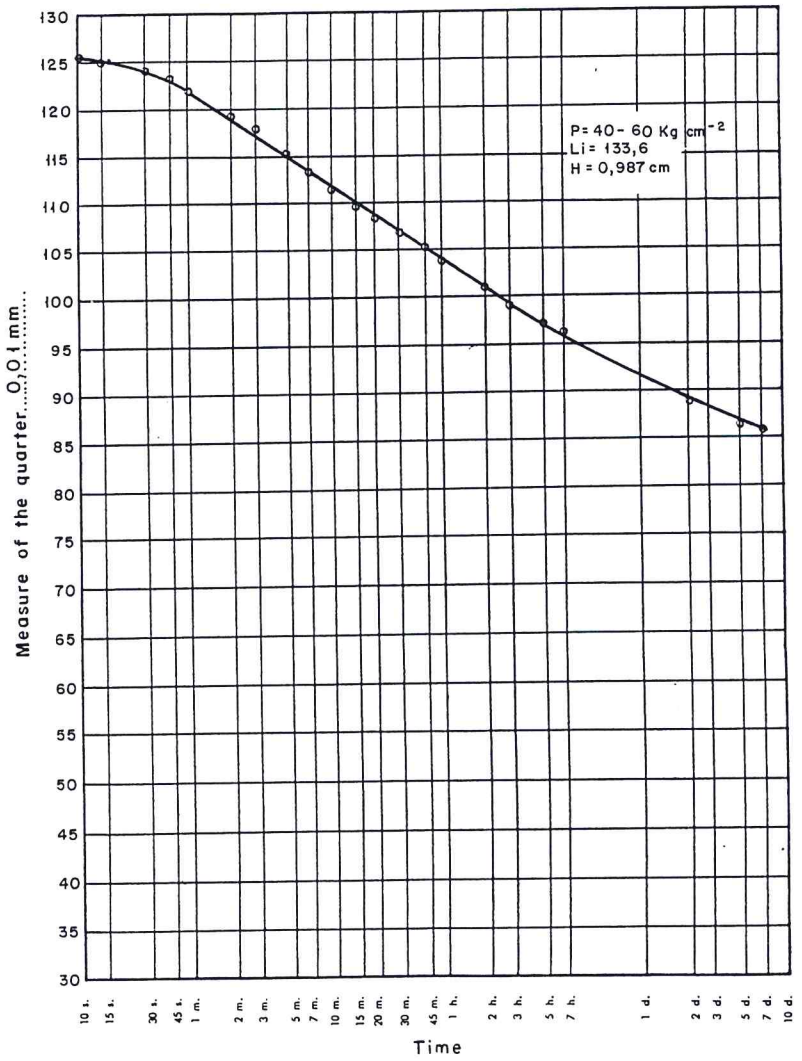

FIG. 31

M - 15 , Clay 75 %

OEDOMETRIC CURVE

Initial dry density: 1,63 Initial moisture: 2,3 Specific weight of the particles 2,755

Initial pore index: 0,780 Final moisture: 23,5 Sample diameter (cm): 7,07 cm

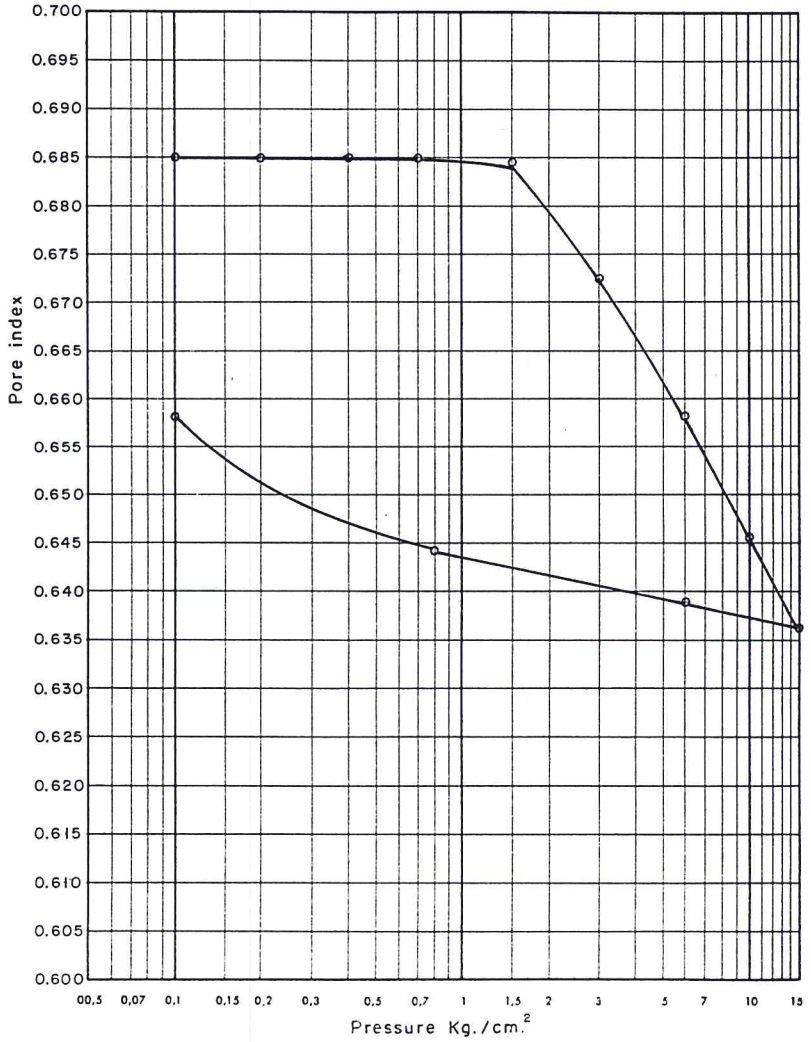

FIG. 32

M-15 , Clay 75 %, ρ_d = 1.63 g cm^{-3}

CONSOLIDATION CURVES

Initial measure of the quarter with null load:.....500..... Edometer height:..12 mm..

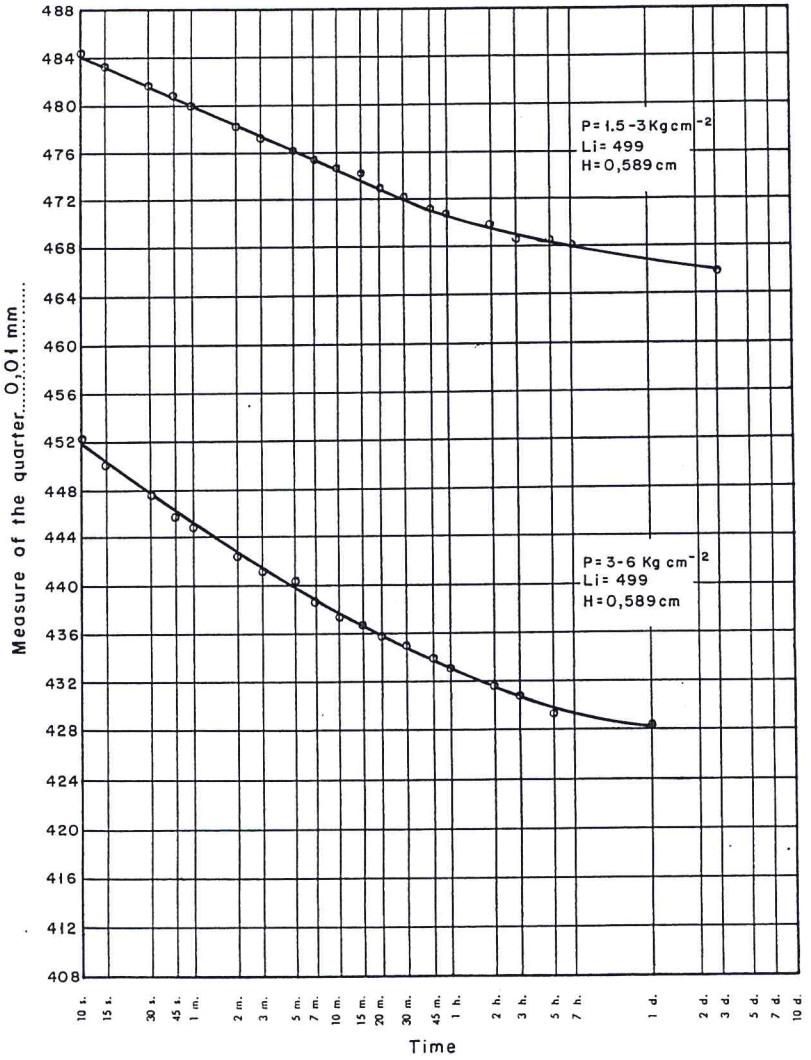

FIG. 33

CONSOLIDATION CURVES

Initial measure of the quarter with null load:....500..... Edometer height:..12 mm..

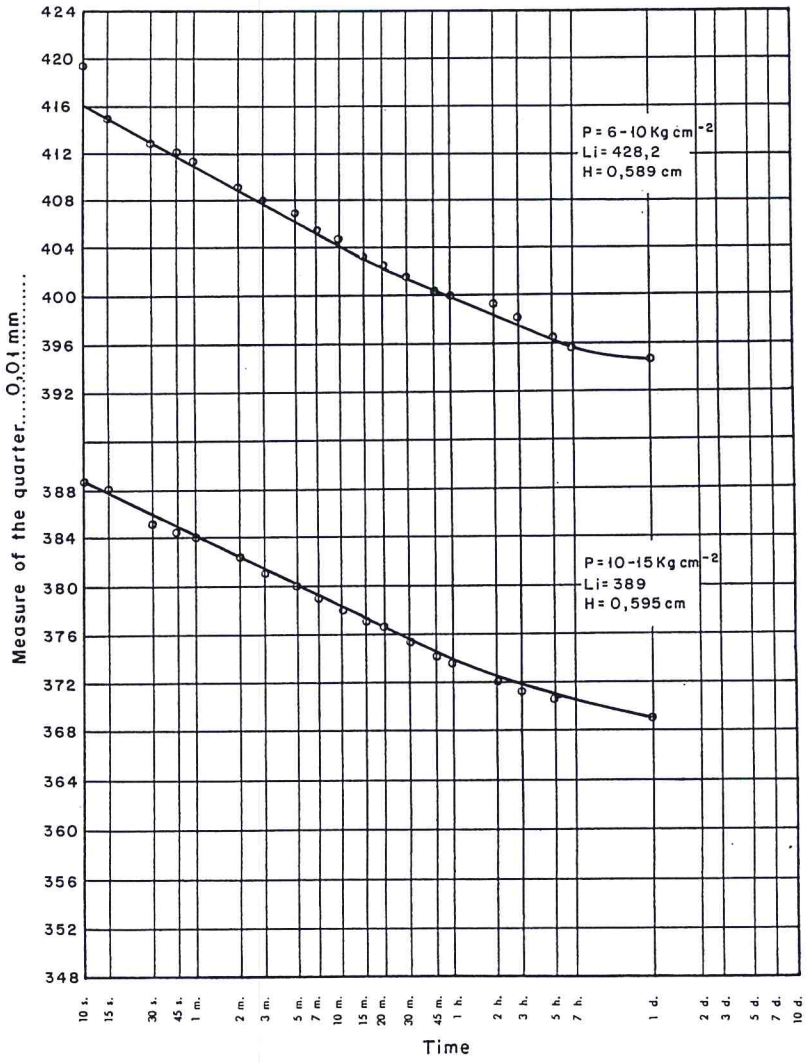

FIG. 34

M - 26 , Clay 100 %

OEDOMETRIC CURVE

Initial dry density: 1,59 Initial moisture: 9,0 Specific weight of the particles 2,478

Initial pore index: 0,548 Final moisture: 73,2 Sample diameter (cm): 2,03

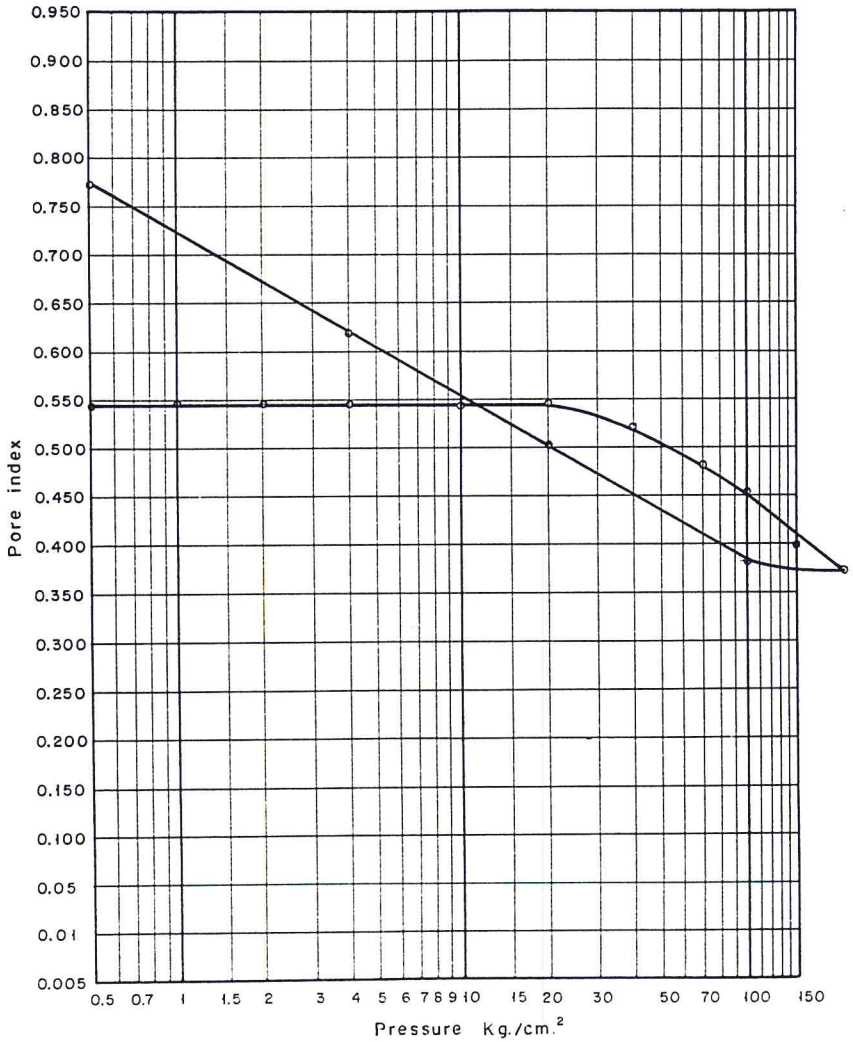

FIG. 35

M - 26 , Clay 100 % , ρ_d = 1,59 g cm^{-3}

CONSOLIDATION CURVES

Initial measure of the qaarter with null load: 500 Edometer height: 12 mm

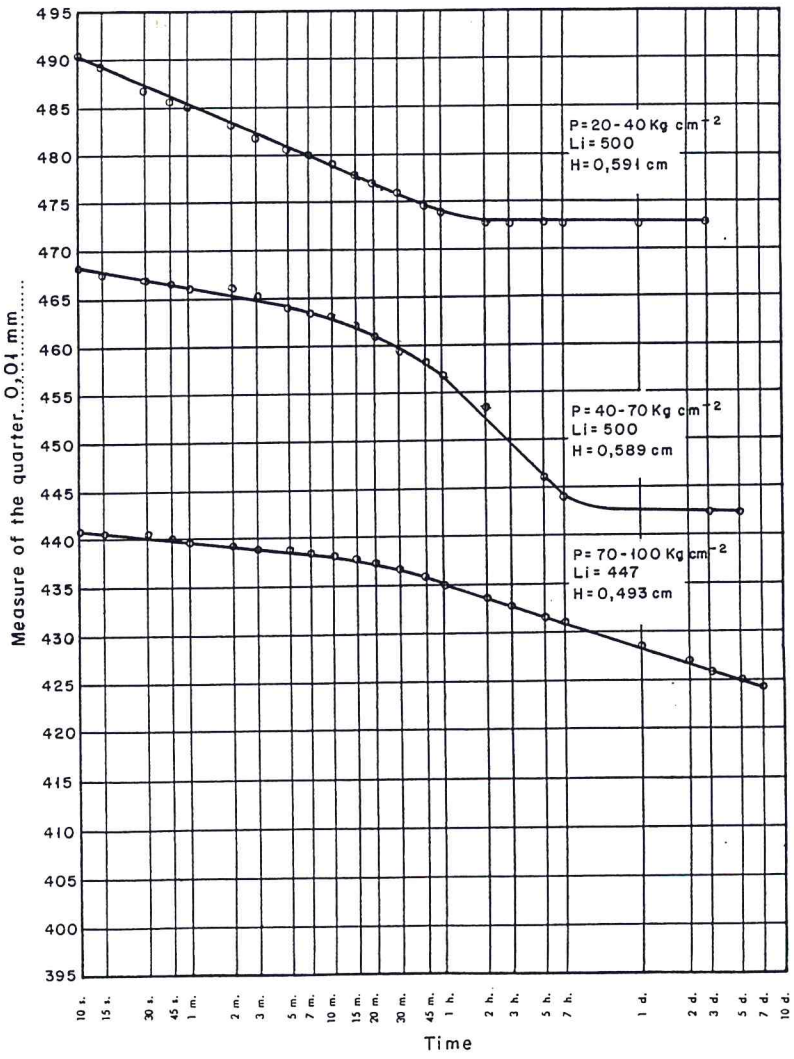

FIG. 36

M - 26 , Clay 100 %, ρd = 1.59 g cm^{-3}

CONSOLIDATION CURVES

Initial measure of the quarter with null load: 500 ..... Edometer height: 12 mm

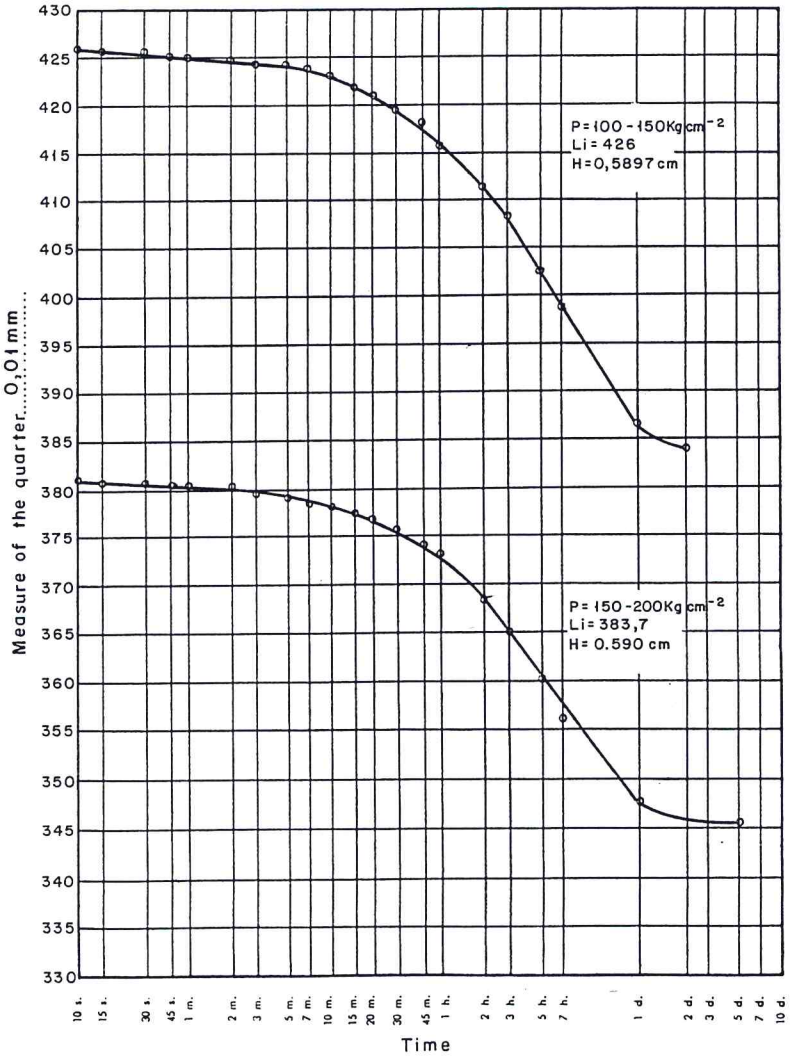

FIG. 37

M - 26 , Clay 75 %

OEDOMETRIC CURVE

Initial dry density: 1,59 ..... Initial moisture: 8,8 ..... Specific weight of the particles: 2,478

Initial pore index: 0,556 Final moisture: 34,9 .. Sample diameter (cm): 3,535 .....

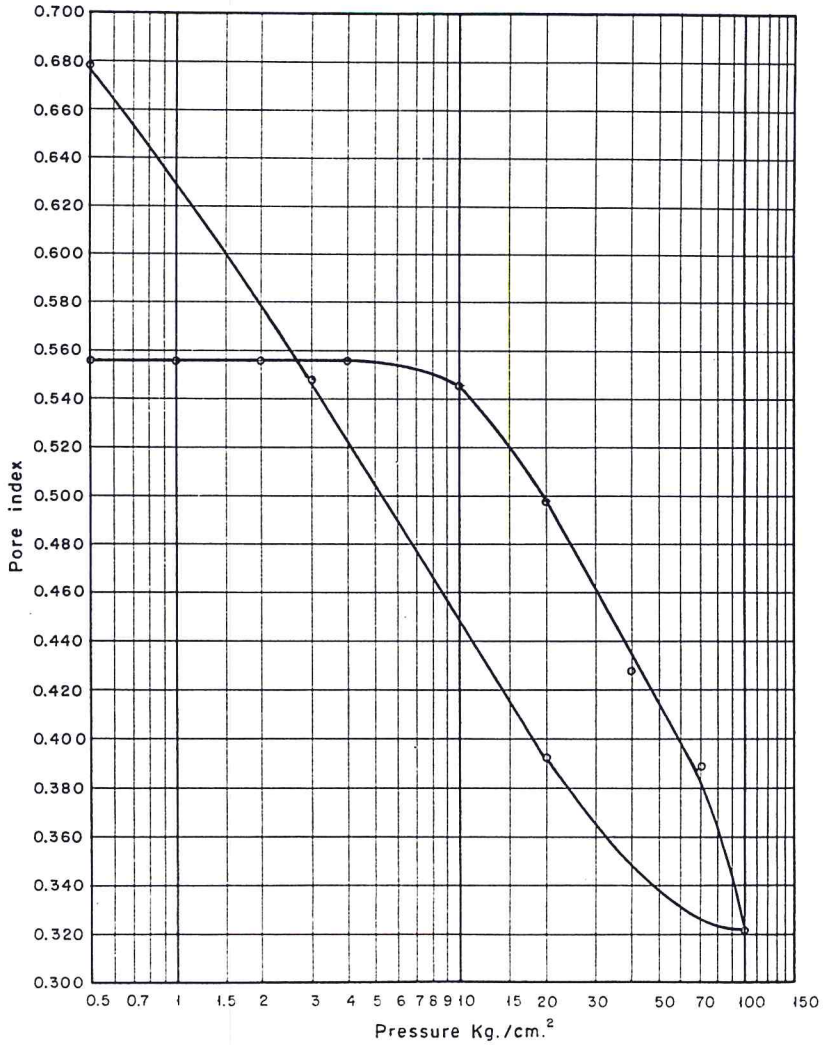

FIG. 38

M - 26 , Clay 75 %, $\varrho d = 1{,}59$ g cm^{-3}

CONSOLIDATION CURVES

Initial measure of the quarter with null load:....500..... Edometer height:..12 mm...

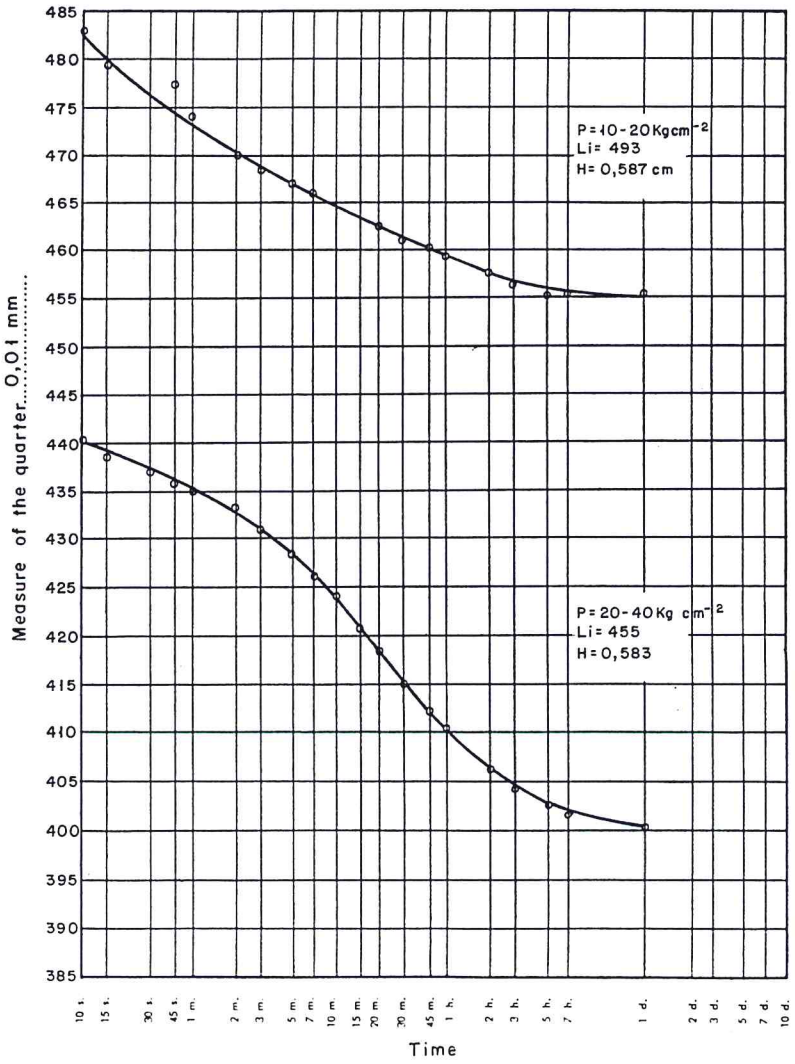

FIG. 39

M - 26 , Clay 75 %, $\varrho d = 1{,}59$ g cm^{-3}

CONSOLIDATION CURVES

Initial measure of the quarter with null load:....500..... Edometer height:..12 mm...

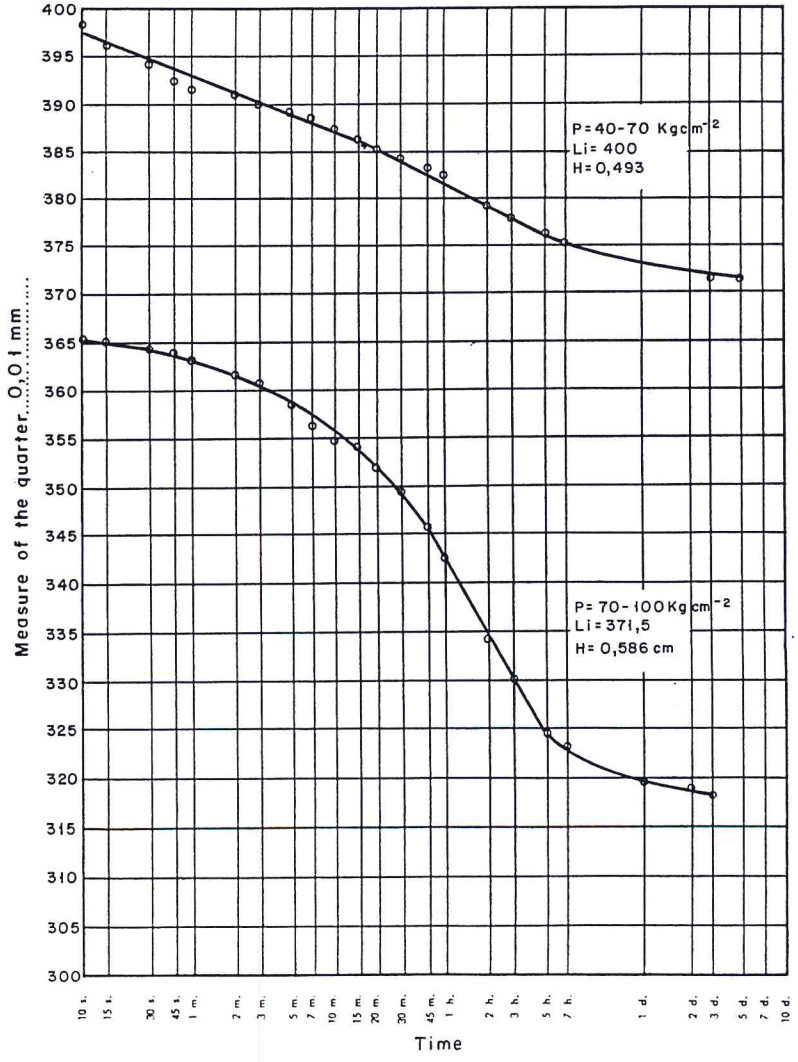

7. MIGRATION EXPERIENCES.

7.1. DISTRIBUTION COEFFICIENTS OF ^{137}Cs AND ^{60}Co.

The retention capacity of radionuclides is another important characteristic of the engineering barriers to be taken into account. To estimate this capacity, the determination of the distribution coefficient of ^{137}Cs and ^{60}Co has been carried out in the montmorillonitic and illitic samples (M-26 and M-15, respectively), as well as in their mixtures with different proportions of granite.

Determinations with ^{236}Pu and ^{243}Am are being done, as well as diffussion tests with compacted blocks of clay and clay - granite mixtures.

The results, presented in this report, have been obtained by using a batch methodology under oxic conditions and with traced water of El Berrocal granitic mine. The solid-solution contact time has been 14 days. Centrifugation at ≃ 30000 g has been used to separate the liquid phase from the solid.

The radionuclide concentration in the solid has been determined by calculating the difference of activity between the initial and final solutions. The distribution coefficient was calculated according to the equation:

$$Rd = \frac{A_i - A_f/W}{A_f/V}$$

Where:

A_i = initial activity
A_f = final activity
W = solid weight (g)
V = liquid volume (ml)

The results are shown in Table XIV, XV and XVI

TABLE XIV
Distribution Coefficients of Cs-137 and Co-60 in the Clay-Granite mixtures*

% Clay	Distribution Coefficient [Rd] (ml/g)			
	Montmorillinite-granite		Illite-granite	
	Cs-137	Co-60	Cs-137	Co-60
100	4249 σ=360	713 σ=51	3399 σ=326	753 σ=24
75	4007 σ=384	687 σ=76	4161 σ=169	767 σ=25
50	3177 σ=282	723 σ=45	4078 σ=152	718 σ=59
25	2012 σ=257	714 σ=78	2971 σ=325	702 σ=88

* $A_i = 2.4 \times 10^5$ Bq/l

TABLE XV
Influence of pH on the Distribution Coefficient of Cs-137 and Co-60

pH	Distribution Coefficient [Rd] (ml/g)			
	Montmorillonite (M-26)		Illite (M-15)	
	Cs-137	Co-60	Cs-137	Co-60
4.9	3369 σ=523	702 σ=143	3380 σ=273	729 σ=101
7.9	4165 σ=218	713 σ= 51	3399 σ=326	753 σ= 24
9.0	4161 σ=260	774 σ=110	4249 σ=236	826 σ=100

The distribution coefficient of ^{137}Cs decreases in the montmorillonite-granite mixture as the clay content decreases.

However. for the illite-granite mixture, the highest values correspond to those mixtures with 75% and 50% illite. The Rd for ^{60}Co are not significant.

An alkaline pH favours the retention capacity of the studied clays.

TABLE XVI
Influence of the initial concentration on the Distribution Coefficients for Cs-137 and Co-60

Ai*	Distribution Coefficient [Rd] (ml/g)			
	Montmorillonite (M-26)		Illite (M-15)	
	Cs-137	Co-60	Cs-137	Co-60
2.56	4031	749	3391	785
11.37	5424	2116	4912	2454
21.99	5301	1983	3999	2611
53.35	2544	1419	1746	1073

* Ai is in KBq/l x 10^5

The influence of other parameters on the distribution coefficient has been analyzed, and a close relation of these values with the experimental condition it is always present. For this reason, new tests will be carried out under "theoretical" conditions, as similar as possible to those expected in the storage site.

7.2. DIFFUSSION ESSAYS.

To get a better understanding of the materials studied as a barrier for the migration of radionuclides, they have been done some diffussion essays that give us information about the dinamic aspects of the retention processes. At the same time these essays get closer to the real conditions that might be expected in a repository, where the composition gradient should be the only parameter that would control the migration phenomena.

The methodology used in these essays has been the following:

- The essays have been done over cylindrical blocks of clay or mixtures clay/granite compacted to densities on the range of 1.8 g/cm^3 and with their saturation moisture.

The dimensions of the compacted blocks are:
ϕ = 3.81 cms.
cross section = 11.4 cm^2
lenght = 7.63 cm
volume = 87 cm^3

- The radioactive tracers were introduced in the blocks during the compactation process; placing, towards the middle of the column, a filter paper impregnated with the solution and dried before being placed in the compacted block.

The concentration for ^{137}Cs has been of 10^{-8} M and for ^{60}Co 10^{-9} M.

- The columns have been confined with a latex casing except in both end that have been isolated with porous materials (filtrating frits). This has allowed the exchenge of humidity with the water saturated atmosphera in which they have been maintained during the essay. The duration of these essays it has been set between 195 and 230 days.

- The analysis of the radionuclide content it has been done over transversal sections of the columns with an approximated average thickness of 1.5 mm. They have been counted for gamma activity with a well-type detector in the energy ranges that are characteristic of ^{137}Cs (632 KeV) and ^{60}Co (1333 KeV).

The experimental results are shown in Figures 40 to 44 (a and b) in which are represented the values of the concentration ratio (C/C_o) vs. the lenght of the column and their accumulated curve.

The analysis of the results it hes been done on the hypothesis that the mobilisation of the radionuclides has been exclusively a diffussion process in the porous media studied; and that this mechanism woulb be basically determined by the ionic diffussion in the aqueous phase, the phenomena of sorption and surface mobility in the solid and the interrelation of pores in the media. Therefore we are measuring an apparent diffussivity; that in the event of one-dimensional diffussion would be expressed by the equation:

$$\frac{dC}{dt} = \frac{\partial}{\partial x}\left(D_a \frac{dC}{dx}\right)$$

In the essay conditions used in our experiment; with a planar source term normal to the diffussion direction andconsidering the column as an infinite cylinder, the previous Eqn. would have the following solution:

$$\frac{C}{M} = \frac{0.5}{(\pi D_a t)^{-0.5}} * e^{-\frac{x^2}{4D_a t}}$$

where:

C = concentration (moles/m^3)

M = total amount of diffussing substance added per unit area (moles/m^2)

x = distance from source (m)
D_a = apparent diffussivity (m^2/s)
t = time (s)

Taking logaritms on this equation we obtain the following expression:

$$\log C = A - B \log x^2$$

where the constants A and B are:

$$A = \log M^* \left[\frac{0.5}{(\pi \, Da \, t)^{-0.5}} \right]$$

$$B = \frac{0.43}{(4D_a t)}$$

In this way the apparent diffussivity coefficient can be obtained from the analysis of the lineal regression log C vs $\log x^2$.

The results of this analysis are shown in Figures 45 to 49 (a and b) and in table XIX

From these results it can be deduced that the addition of granite slightly increases the apparent diffussion in montmorillonite for both radionuclides, ^{127}Cs and ^{60}Co. For the illite the D_a coefficient slightly decreases with the addition of 50% of granite, but it can not be stablished a trend for this clay due to a lack of data, because the programmed essay with 75% of granite was not properly done.

TABLE IV
DIFFUSSION ESSAYS: PARAMETERS AND CALCULATED DIFFUSSIVITY COEFFICICENTS

Sample	log Ci		Time (days)	Apparent Diffussivity (Da) (m^2/s)
	Cs-137	Co-60		
M-15 100% Clay	-7.21	-8.21	195	Da (Cs) = 1.70 E-13 Da (Co) = 3.01 E-13
M-15 50% Clay	-7.17	-8.17	198	Da (Cs) = 1.00 E-13 Da (Co) = 1.76 E-13
M-26 100% Clay	-7.11	-8.15	217	Da (Cs) = 1.60 E-13 Da (Co) = 2.16 E-13
M-26 50% Clay	-7.09	-8.15	223	Da (Cs) = 4.91 E-13 Da (Co) = 6.51 E-13
M-26 25% Clay	-7.09	-8.08	230	Da (Cs) = 5.88 E-13 Da (Co) = 7.09 E-13

For the small variations of the determined diffussion coefficient (D_a), the addition of granite would improve slightly the behaviour of the illite while it would have the opposite effect in montmorillonite.

In Fig. 50 it has been represented the variation of the apparent diffussion coefficient versus the granite content of the mixtures.

Fig.1a.- Diffussion profile of Cesium
Illite M-15 pure
Diffussion time = 195 days

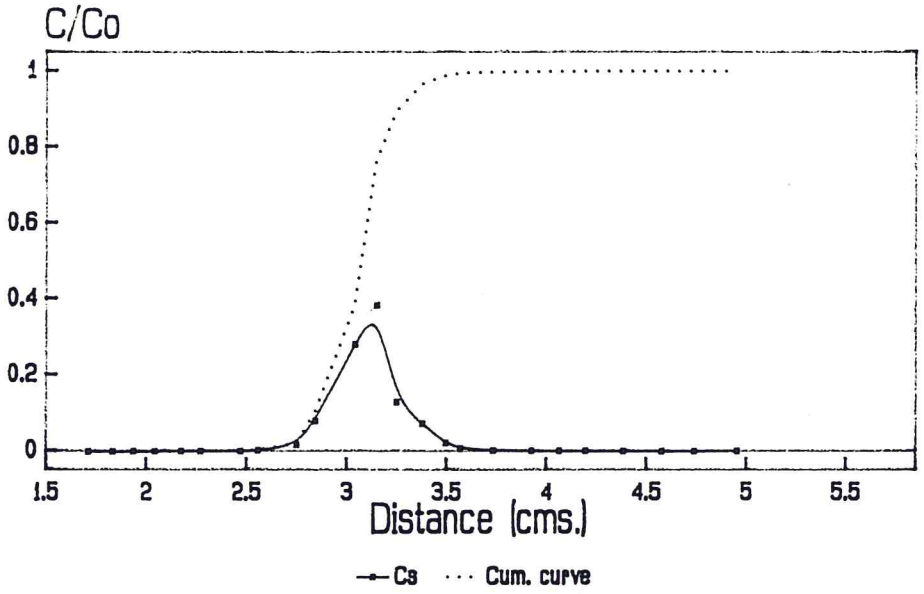

Cesium conc. = 6.15 E-8 M

Fig.1b.- Diffussion profile of Cobalt
Illite M-15 pure
Diffussion time = 195 days

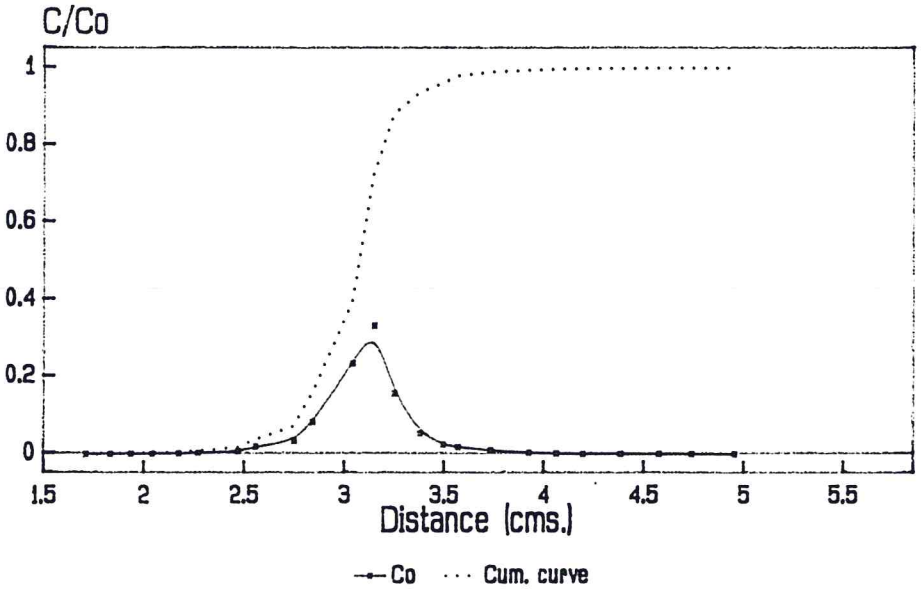

Cobalt conc. = 6.05 E-9 M

Fig 2a.- Diffussion profile for Cesium
50% Illite M-15 + 50% granite
Diffussion time = 198 days

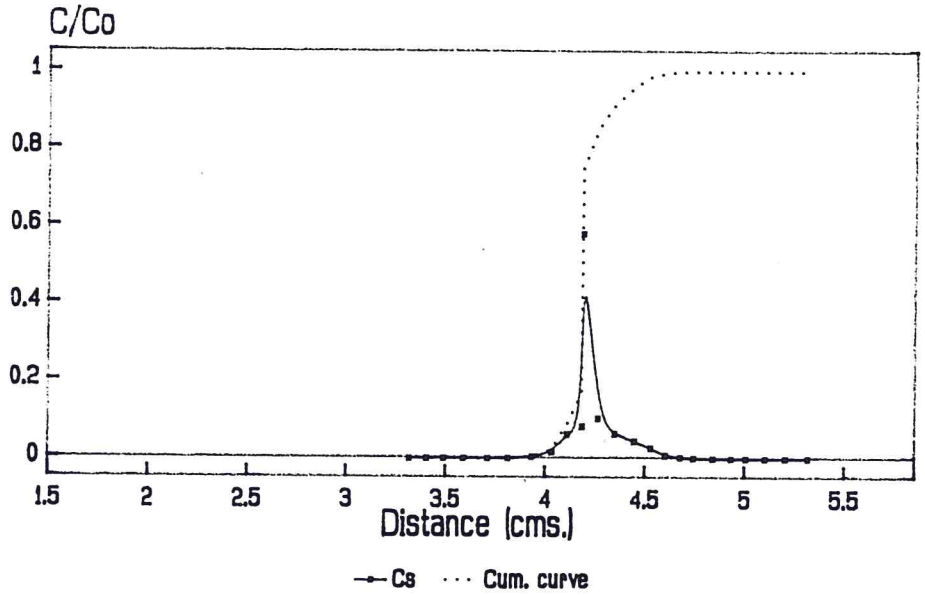

Cesium conc. = 7.34 E-8 M

Fig 2b.- Diffussion profile for Cobalt
50% Illite M-15 + 50% granite
Diffussion time = 198 days

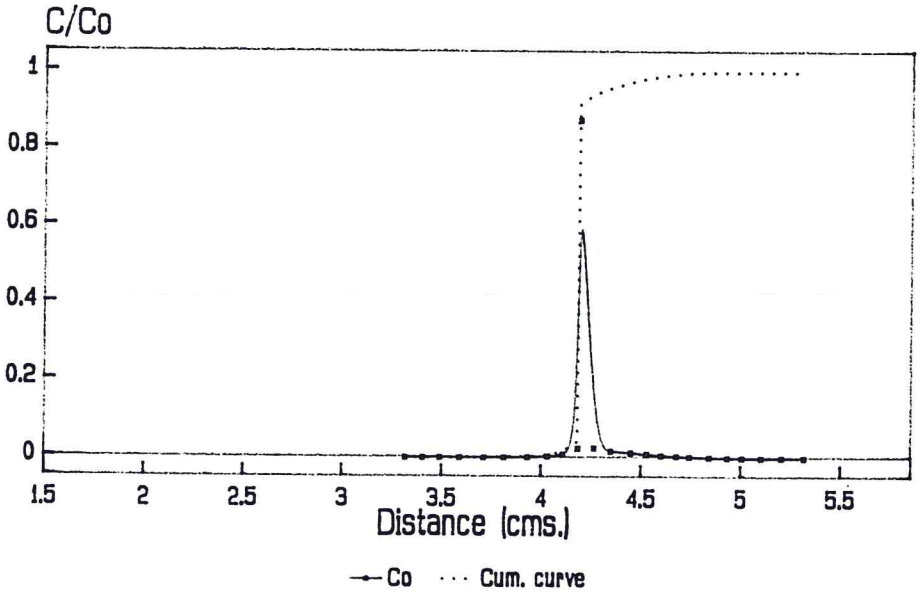

Cobalt conc. = 6.68 E-9 M

Fig. 3a.- Diffussion profile for Cesium
Montmorillonite M-26 pure
Diffussion time = 217 days

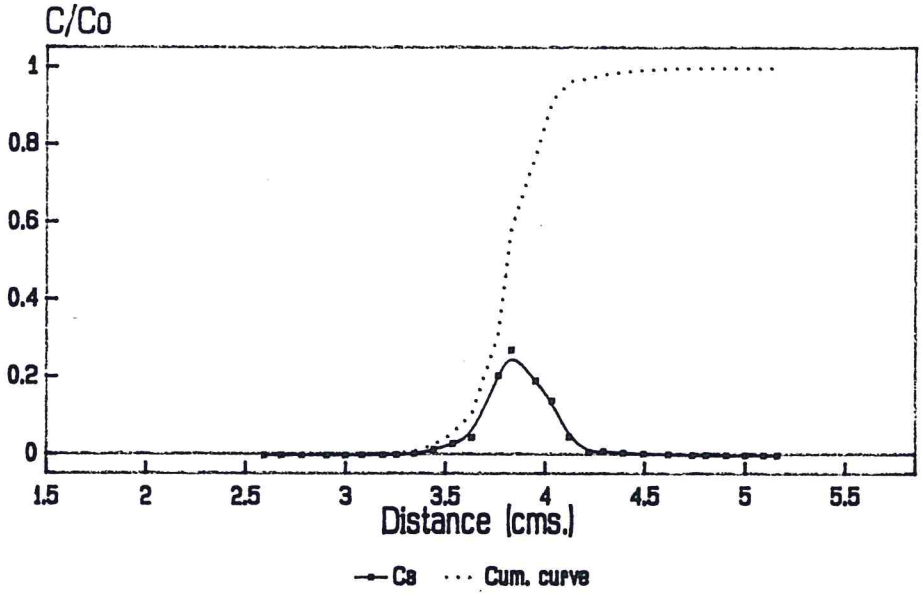

Cesium conc. = 7.83 E-8

Fig. 3b.- Diffussion profile for Cobalt
Montmorillonite M-26 pure
Diffussion time = 217 days

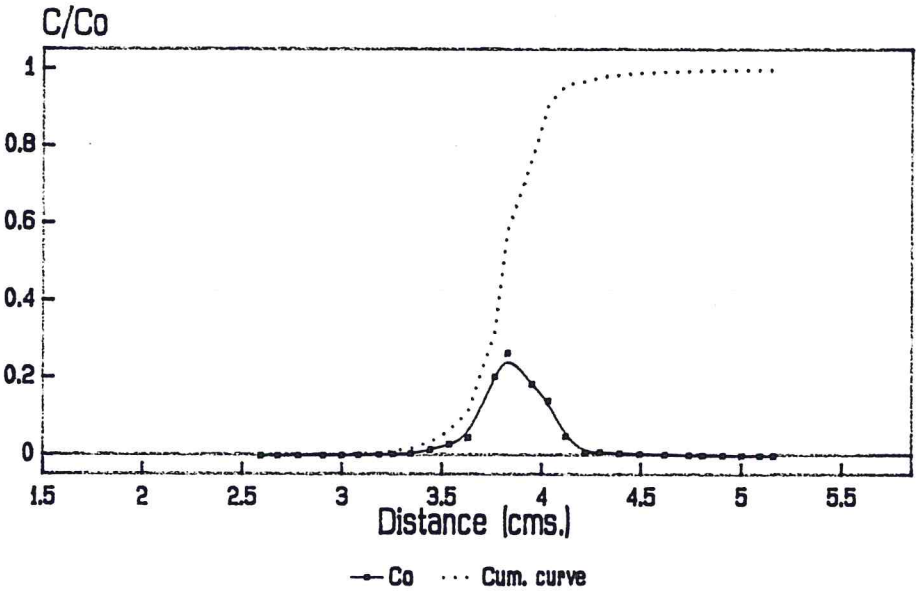

Cobalt conc. = 7.00 E-9

Fig. 4a.- Diffussion profile for Cesium
50% Montmorillonite M-26 + 50% granite
Diffussion time = 223 days

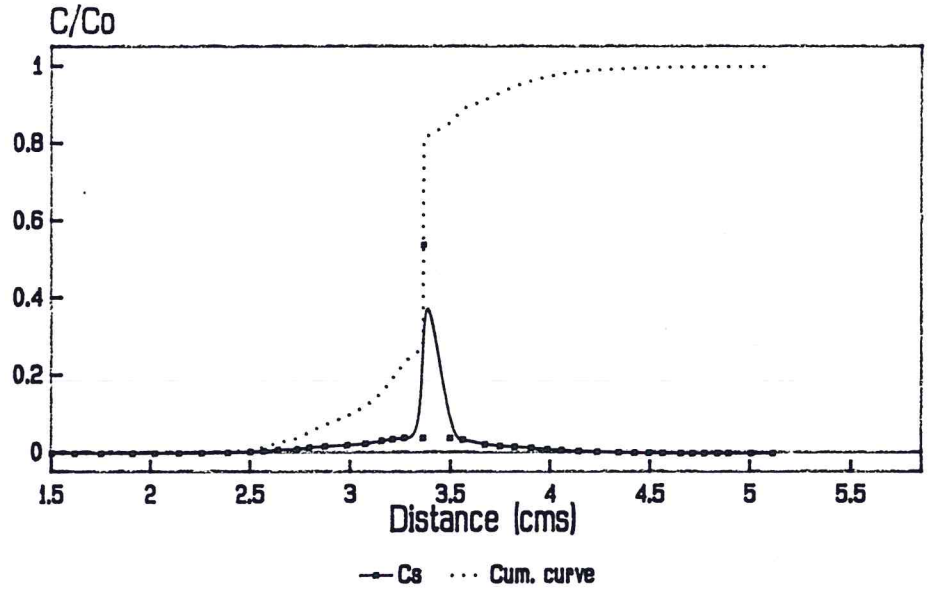

Cesium conc. = 8.17 E-8 M

Fig. 4b.- Diffussion profile for Cobalt
50% Montmorillonite M-26 + 50% granite
Diffussion time = 223 days

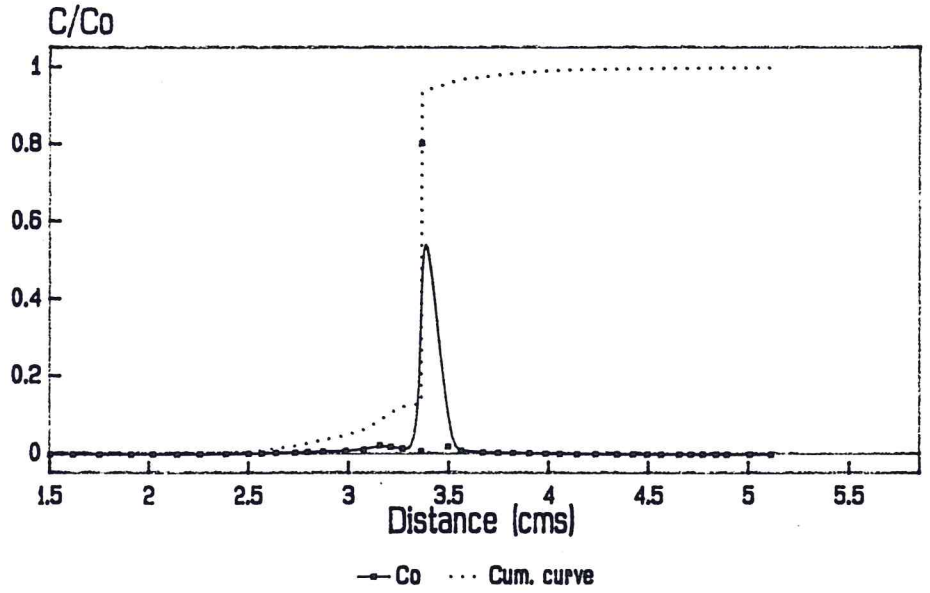

Cobalt conc. = 7.05 E-9 M

Fig. 5a.- Diffussion profile for Cesium
25% Montmorillonite M-26 + 75% granite
Diffussion time = 230 days

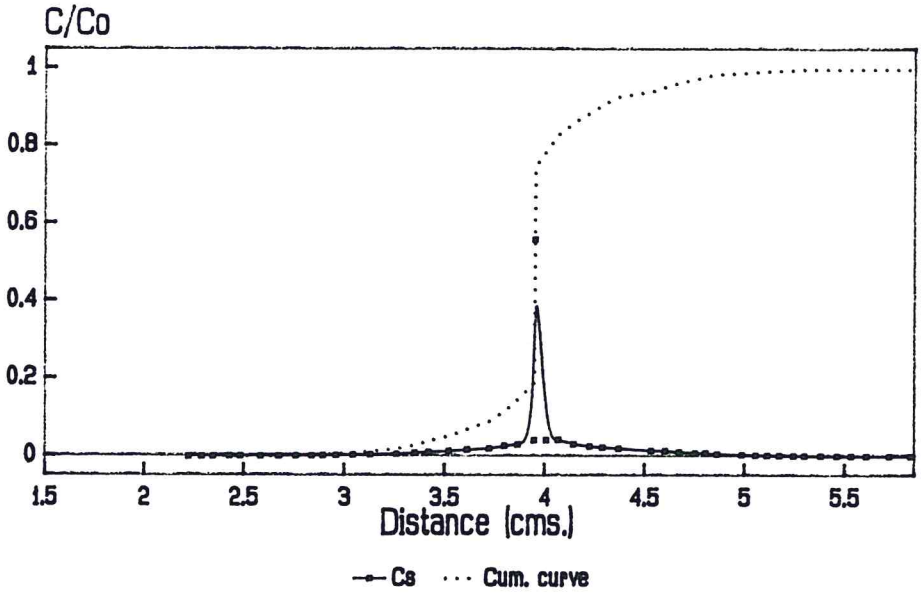

Cesium conc. = 8.18 E-8 M

Fig. 5b.- Diffussion profile for Cobalt
25% Montmorillonite M-26 + 75% granite
Diffussion time = 230 days

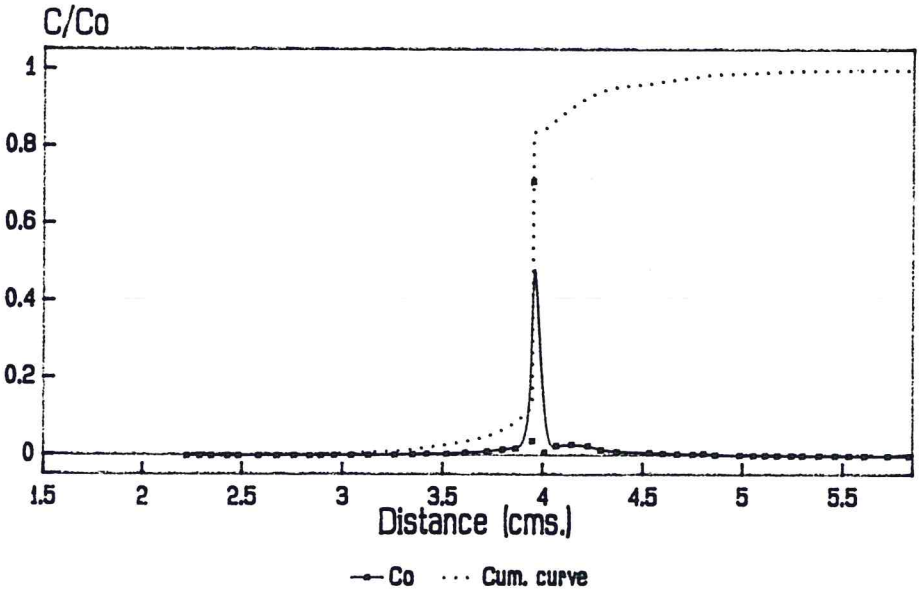

Cobalt conc. = 8.31 E-9 M

Fig. 1c.- Diffussion of Cesium in clay
100 % of Illite M-15

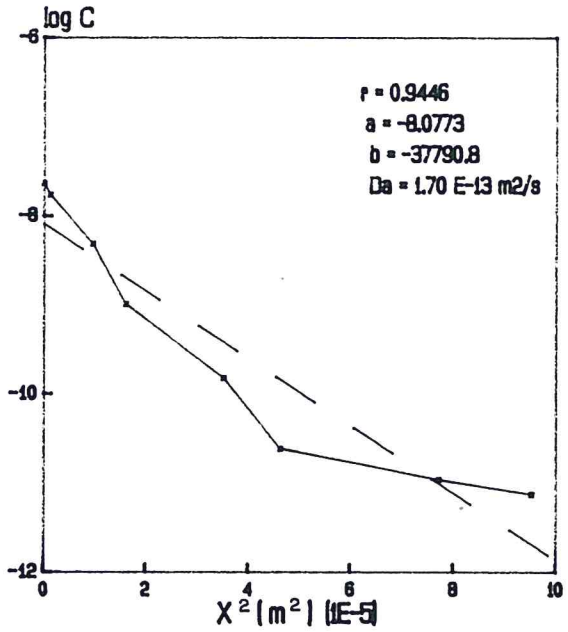

Diffussion time = 195 days

Fig. 1d.- Diffussion of Cobalt in clay
100 % of Illite M-15

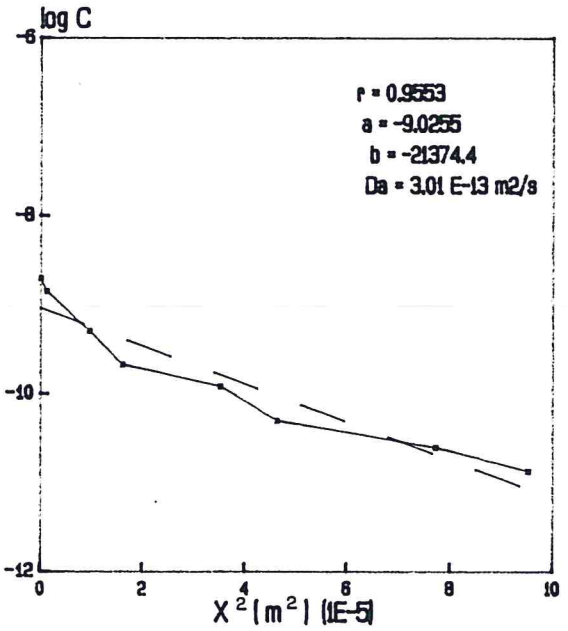

Diffussion time = 195 days

Fig. 2c.- Diffussion of Cesium in clay
50 % of Illite M-15 + 50 % granite

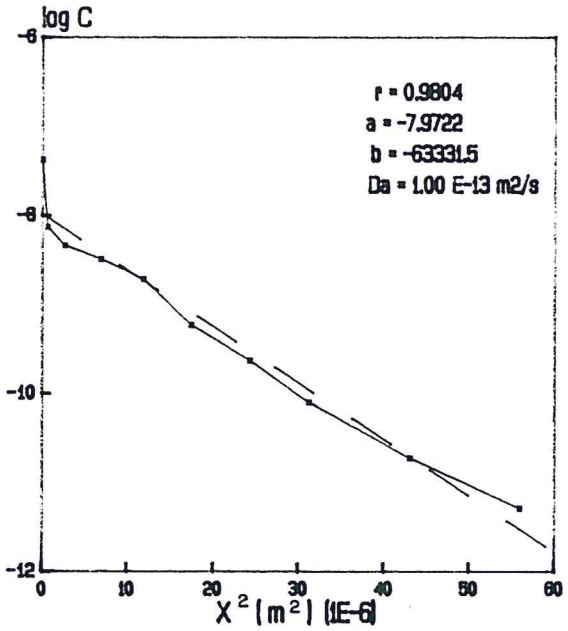

Diffussion time = 198 days

Fig. 2d.- Diffussion of Cobalt in clay
50 % of Illite M-15 + 50 % granite

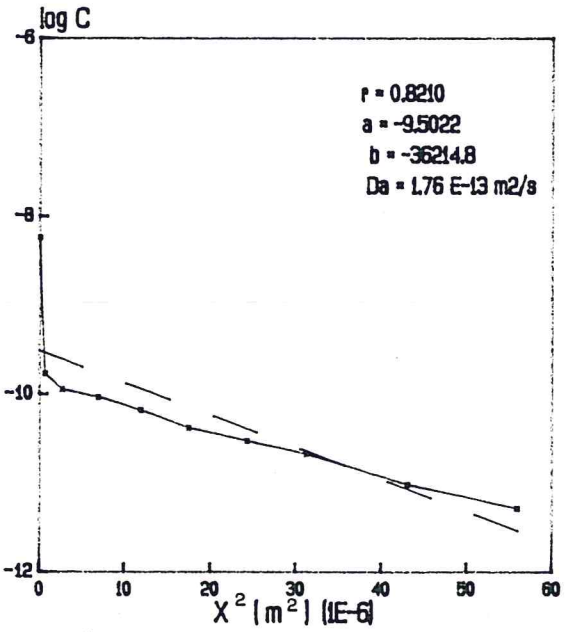

Diffussion time = 198 days

Fig 3c.- Diffussion of Cesium in clay
100 % of Montmorillonite M-26

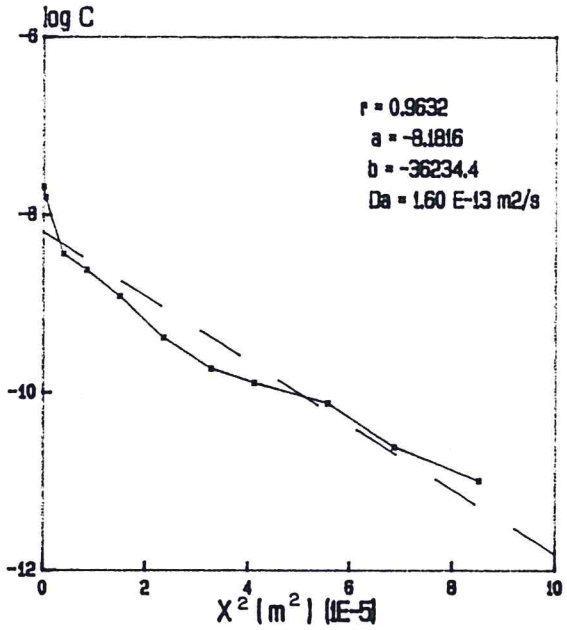

Diffussion time = 217 days

Fig 3d.- Diffussion of Cobalt in clay
100 % of Montmorillonite M-26

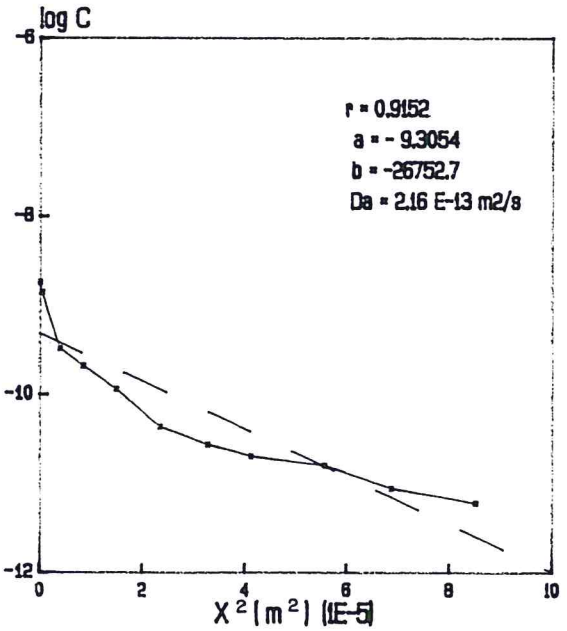

Diffussion time = 217 days

Fig. 4c.- Diffussion of Cesium in clay
50% Montmorillonite M-26 + 50% granite

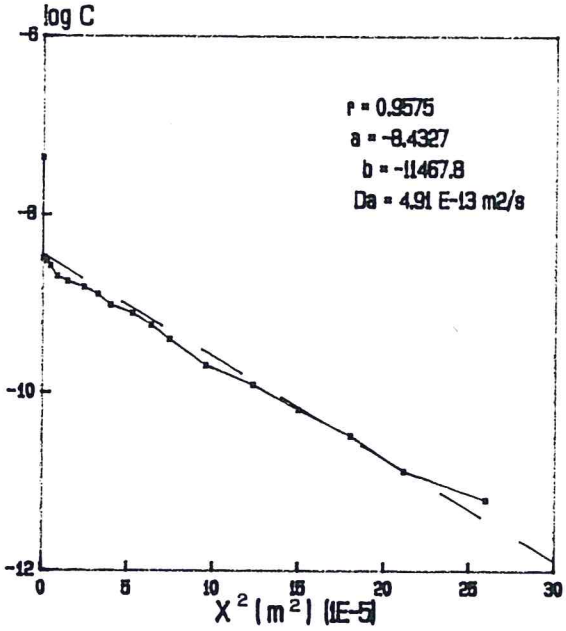

Diffussion time = 223 days

Fig. 4d.- Diffussion of Cobalt in clay
50% Montmorillonite M-26 + 50% granite

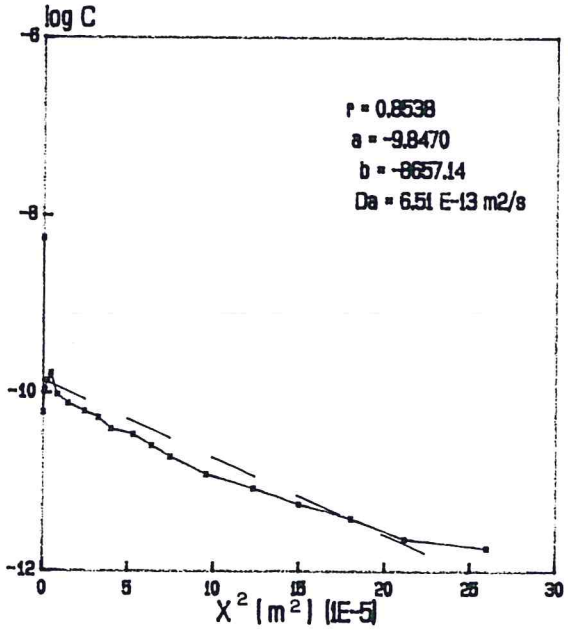

Diffussion time = 223 days

Fig. 5c.- Diffussion of Cesium in clay
25% Montmorillonite M-26 + 75% granite

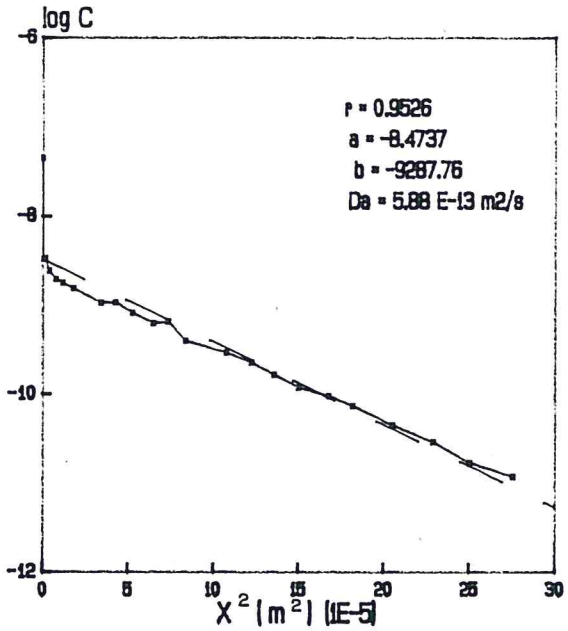

Diffussion time = 230 days

Fig. 5d.- Diffussion of Cobalt in clay
25% Montmorillonite M-26 + 75% granite

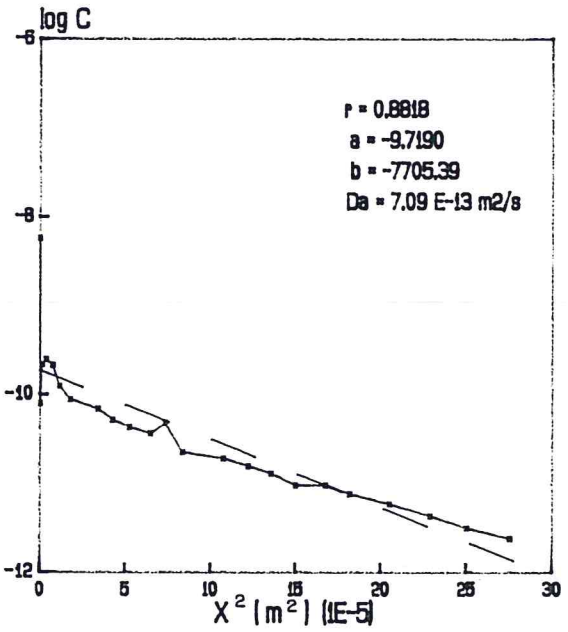

Diffussion time = 230 days

Fig. 50 SAMPLES M-26 & M-15
Apparent Diffusivity vs. clay
content in clay-granite mixtures

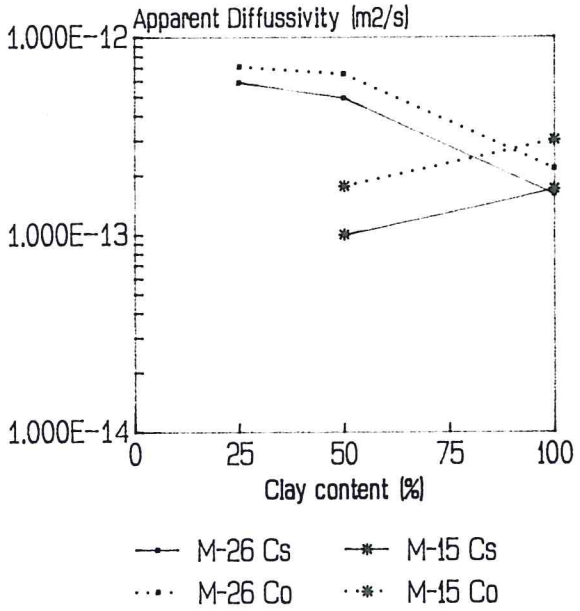

8. THE STABILITY OF MONTMORILLONITE, M-26, AS A FUNCTION OF K^+, TEMPERATURE AND TIME (Preliminary test).

8.1. INTRODUCTION.

According to the mineralogical, geochemical and physico-chemical data, sample M-26 was selected, in previous reports, as the most favorable smectite to meet the goal of this project.

This sample is essentially constituted by smectite (94%), quartz, plagioclase, calcite and amorphous substances.

This report summarizes the first results of the tests carried out on the stability of the smectite in relation to K^+, temperature and time. The purpose of these tests is to know the transformations of the smectite as it is altered to illite.

8.2. MATERIALS AND METHODOLOGY.

8.2.1. Smectite.- In the tests, the fraction x <2 um of sample M-26 has been used, which is almost exclusively constituted by smectite ($\simeq$ 99%).

The diffractograms and chemical analyses, like DTA and TG have allowed a more precise identification, in relation to previous reports, of the type of semectite present in sample M-26.

8.2.1.1. Diffractometric characteristics.- These characteristics are summarized in Table XX.

TABLE XX. DIFFRACTOMETRIC CHARACTERISTICS OF x<2um FRACTION OF M-26

XRD	D(001)A	A 001	A 10A	A 17A / A 10A	V/P	d(060)	OBSERVAT.
NO.P.	---	---	---	---	---	1,4955	Dioct.
OA-N	14,71	5600mm^2	---	---	0,95		
OA+EG	16,98	4590mm^2	---	---	---		
OA+300ºC	~10	---	2035	2,255	---		

NO.P Non-oriented powder, OA-N= normal oriented aggregate, OA+EG= =treated with ethylene glycol OA+300ºC= heated at 300ºC for 2 h. d(001)=basal spacing, A (001)= basal reflection area, A~ 10A= area after being heated at 300ºC, A 17A/A 10A = Schultz's illitization index (1978), V/P= Biscaye's crystallinity index (1965).

8.2.1.2. Chemical characteristics and structural formula.- The chemical composition of the studied sample, the cation exchange capacity and the structural formula are represented in Table XXI.

Based on the data of Tables XX and XXI, the smectite of sample M-26 is a Wyoming type montmorillonite, following SCHULTZ'S classification (1969).

8.2.1.3. Thermic and thermogravimetric characteristics..- These characteristics are represented by the curves in Fig. 51.

According to the DTA curve (Fig 51a), the smectite (M-26) shows the thermic characteristics corresponding to dioctahedral smectites, of the "normal" montmorillonite type, according to the terminology used by MACKENZIE (1970). This curve is characterized by a complex endothermic peak, with the main minimun at 143°C, and an accessory one at 195°C. This

endothermic system, whose shape, size and temperature, depends on the exhangeable cation or cations of the montmorillonite, corresponds to a loss of moisture of the montmorillonite. This loss of water is reflected on the TG curve (Fig. 51b) by the interval between 40 and 220ºC, where a loss of 13,04% in weight occurs.

TABLE XXI. CHEMICAL COMPOSITION AND STRUCTURAL FORMULA OF M-26

CHEMICAL COMPOSITION		EXCHANGE CAPACITY (meq/100g)		STRUCTURAL FORMULA		
SiO_2	60.45%			Si(IV)	7.771	-0.219
Al_2O_3	19.29			Al(IV)	0.229	
Fe_2O_3	3.94					
FeO	0.31			Al(VI)	2.694	
MnO	0.03			Fe^{3+}(VI)	0.381	
MgO	6.63	Mg^{++}	30.53	Fe^{2+}(VI)	0.034	-0.343
CaO	0.94	Ca^{++}	29.75	Ti(VI)	0.014	
Na_2O	1.06	Na^{+}	10.27	Mg(VI)	1.154	
K_2O	1.05	K^{+}	3.11			
TiO_2	0.15			Mg^{2+}	0.117	
H_2O^{+}	6.13			Ca^{2+}	0.114	+0.564
				Na^{+}	0.078	
				K^{+}	0.024	
Total	99.98%		73.66	% Tetrahedral charge = 38.97 %		

At approximately 660ºC, there is another endothermic effect which corresponds to the loss of the structural hydroxyl groups of the mineral, and therefore, to the second important loss in weight, which is observed in the TG diagram.

The DTA curve ends with an endothermic effect at 870ºC, followed by another exothermic peak at a temperature above 950ºC, which corresponds to some entropy change of the montmorillonite and to the recrystallization of new mineral phases, respectively.

In the TG curve (Fig 51b), a gradual and continuous loss of weight between the two most important peaks is observed, and it is due to the loss of structural OH^- groups, which starts before the total loss of hydration water is accomplished. This fact, that depends on the nature of the exchangeable cation or cations, is only observed when these have a high hydration energy (like Ca^{++} and Mg^{++}).

Finally, the loss of weight continues after the second important peak in the TG curve, also in a gradual way, though more slowly than in the preceding region. This fact can be explained by considering that the structural OH^- groups are also gradually released after the above mentioned peak.

The temperature displacements, observed between the DTA and TG curves, are due to the different heating speed at which these tests have been carried out.

8.2.2. The reagent.- A solution of Merck's KCl 0,1M has been used in the tests. The pH of the solution is 5,52.

8.2.3. The reactive vessel.- It is made of stainless steel, with a double entry, and a volume of 25 cc, having the inner part lined with teflon. The model is similar to the one described by ATABEK et al (1987).

8.2.4. Experimental conditions.- The conditions, under which the alteration tests were carried out, are summarized in Table XXII.

The time of reaction is the only condition that has been modified.

TABLE XXII REACTION CONDITIONS

TESTS	Solid	Solution KCl 0,1M	mg K/liq sol/liq		T°C	Time days
1st	3g	15cc	58,65	1:5	175°C	30
2nd	3g	15cc	58,65	1:5	175°C	60
3rd	3g	15cc	58,65	1:5	175°C	90

8.2.5. Analyses carried out after the reaction

a) On the resulting solid.- X.R. diffraction (OA-N, OA+EG, OA+300°C).

b) On the resulting solution.- Chemical analyses of SiO_2 and P_2O_5 by colorimetry; K by flame emission spectrometry, and Al, B, Ba, Ca, Fe, Mg, Mn, Na, Sr, Ti, and Zn by ICP.

8.3.1.1 Diffractometric results.- These results, which are represented in Table XXIII, are compared with the ones corresponding to the non-treated montmorillonite.

According to the data in this table, the following can be deduced:

a) The basal spacing of the hydrated montmorillonite and the one treated with ethylene glycol decreases as the time in contact with a KCl solution 0,1M increases.

b) The relation of the basal reflection area of the montmorillonite treated with ethylene glycol (≃ 17A) and the area of the same reflection of the montmorillonite heated at 300ºC (SCHULTZ'S illitization index, 1978), decreases from the natural montmorillonite to the one treated with KCl. This relation is practically constant in the three test.

c) BISCAYE'S crystallinity index (1965) varies from 0,95, in the natural montmorillonite, to 1 in those treated with KCl, being this value constant in the three test.

8.3.1.2. Thermic behavior of the resulting solid.- Though there are no DTA curves, the TG curves and their respective derivatives (Fig. 52) are clear enough as to deduce that the montmorillonite, after the three tests, has not suffered important changes detectable by this technique.

8.3.1.3. Chemical composition of the resulting solution.- Table V shows the concentration of the chemical elements found in the solution, expressed in mg/15 cc. Likewise, these values have been referred to the solid (ppm) to give an idea of the amounts leached from it. Besides, the cation exchange complex and the K^+ fixed in the montmorillonite, expressed in meq/100 gr., are also represented in the table.

TABLE XXIV. POST-REACTION CHEMICAL COMPOSITION OF THE RESULTANT SOLUTION

	IN THE SOLUTION			REFERRED TO THE SOLID			EXCHANGE CATIONS			K FIXED BY MONT.		
	30 days mg/15cc	60 days mg/15cc	90 days mg/15cc	30 days (ppm)	60 days (ppm)	90 days (ppm)	30 days meq/100g	60 days meq/100g	90 days meq/100g	30 days meq/100	60 days meq/100	90 days meq/100
SiO_2	64,6	143,3	144	323	716	720	---	---	---			
K	21,25	21,25	17,5	---	---	---	---	---	---	31,89	31,89	42,20
Na	485	500	496	2425	2500	2480	10,54	10,87	10,78			
Ca	205	225	365	1025	1125	1825	5,13	5,62	9,13			
Mg	114	125	140	570	625	700	4,75	5,21	5,83			
Ba	0,8	1,1	1,4	4	5,5	7	0,006	0,008	0,01			
Sr	3,6	3,8	5,5	18	19	27,5	0,04	0,043	0,06			
B	7,8	7,1	3	39	35,5	15	---	---	---			
Mn	0,42	0,71	0,5	2,0	3,5	2,5	---	---	---			
Zn	< 0,5	1,6	< 0,5	< 2,5	8	< 2,5	---	---	---			
Fe	< 0,5	< 0,5	< 0,5	< 2,5	< 2,5	< 2,5	---	---	---			
Al	< 0,8	< 0,8	2,4	< 4	< 4	12	---	---	---			
Ti	< 0,5	< 0,5	< 0,5	< 2,5	< 2,5	< 2,5	---	---	---			
P_2O_5	50	< 50	< 50	250	< 250	< 250	---	---	---			
						Total	20,466	21,751	25,81	31,89	31,89	42,20
						Total of charges	30,39	32,63	40,84	31,89	31,89	42,20

The variation of SiO_2 leached from the solid, of the total cation exchange complex (TCEC), of the exchange cations (Na^+, Ca^{++} and Mg^{++}) and of the K^+ fixed by the montmorillonite, as a function of the reaction time, are represented in Fig 53.

8.4. DISCUSSION OF THE RESULTS AND CONCLUSIONS

Based on the results from Table XXIV and from their plots, the following is deduced:

a) Only a partial cation exchange of the montmorillonite has been achieved in the three tests.

b) The only cation which has been totally replaced by K^+ is Na^+, replacement which is accomplished in 30 days and in the same way than under normal temperature conditions.

c) Ca^{++} and Mg^{++} have been replaced only in a small proportion. That is, 30.69% and 19.1% of the available Ca^{++} and Mg^{++} at the most, respectively.

d) In relation to Ca^{++}, the amount replaced by K^+ suddenly increases after 90 days, while the amount of Mg^{++} increases very slowly with time.

The different behavior of these cations depends on their different diameter, bigger for Ca^{++} than for Mg^{++}, for equal charges.

In fact, in the tests carried out, the generally admitted replacing power is maintained, being the following: $Na^+ < K^+ < Ca^{++} < Mg^{++}$. This means that K^+ replaces Na^+ more easily than it replaces Ca^{++} and Mg^{++}.

On the other hand, the fact that a total cation exchange has not been achieved, in spite of the existence of K+ in the solution, is also due to the relatively low K^+ concentration in the original solution (0.1 M). Nevertheless, and taking the behavior of Ca^{++} into account, it is presumable that with a longer time of reaction, the exchangeable amount of Ca^{++}, and even Mg^{++}, would increase.

e) Besides Na^+, Ca^{++} and Mg^{++}, Ba^{++} and Sr^{++} have been detected in the resulting solution. These cations can be adsorbed by the montmorillonite, thus neutralizing the unsatisfied charges present around the edges of the smectite particles. These free charges are due to broken bonds in the silica-alumina layers.

f) The differences observed in the charge balance during the three ion exchange processes are probably due to the manipulation of the samples, before and after the reaction, and/or to analytical errors. Anyway, the differences can be considered within the error limit of the method.

g) Besides the exchange cations, SiO_2 is the solid component which is leached in significant amounts. Thus, the amount of SiO_2 increases lineally from the first to the second test, and stabilizes itself in the third one. This dissolved silica comes from the amorphous silica contained in the sample, approximately 1%.

h) As it was stated before, the chemical changes originated in the montmorillonite M-26 do not distinctly affect its thermic behavior. Thus, the presence of two peaks, due to H_2O loss, in the TG derivative curve indicates the persistance of Ca^{++} and Mg^{++}, as exchangeable cations, in

the montmorillonite, ions which have a greater hydration energy than K^+.

i) The introduction of K^+, in exchange position, in the montmorillonite is shown in the XRD by a gradual decrease of the basal spacing of the montmorillonite. This is due to the less amount of hydration H_2O of the montmorillonite, which is a consequence of the partial substitution of Ca^{++} and Mg^{++} by K^+, fundamentally.

j) BISCAYE'S crystallinity index (1965) increases slightly from the non-treated montmorillonite to the treated one. This index does not vary along the three tests. SCHULTZ'S illitization index (1978), which, according to this author, varies from 4.7, for pure smectites, and 0 when the illitic layers increase, do not seem to have any meaning in our case.

In short, the tests carried out on the montmorillonite M-26 have only originated a partial cation exchange process.

If any illite has been produced in the smectite, it has not been detected with the analytical techniques used in this study.

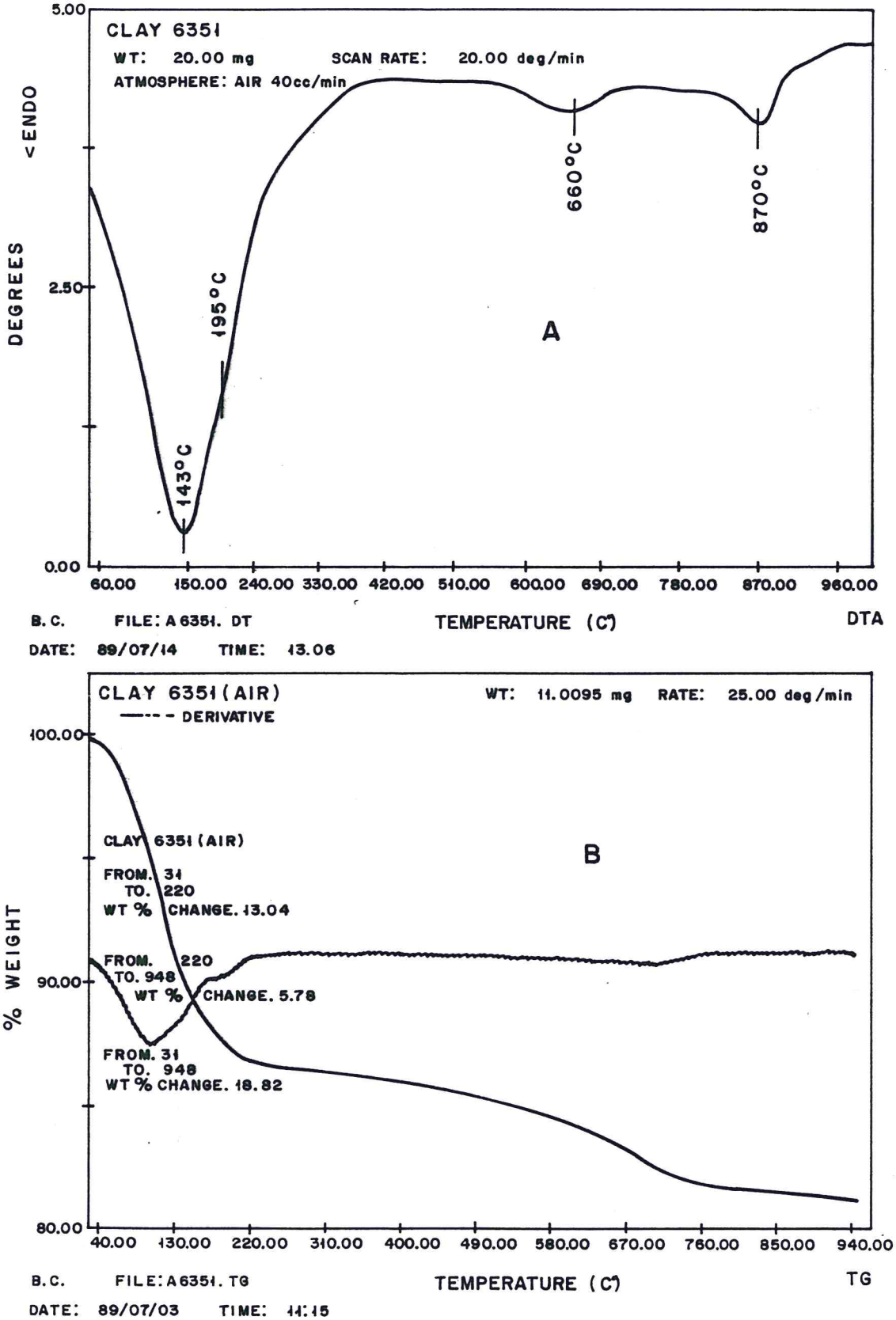

FIG. 51. DTA and TG curves of the $x < 2\,\mu m$ fraction of sample M - 26.

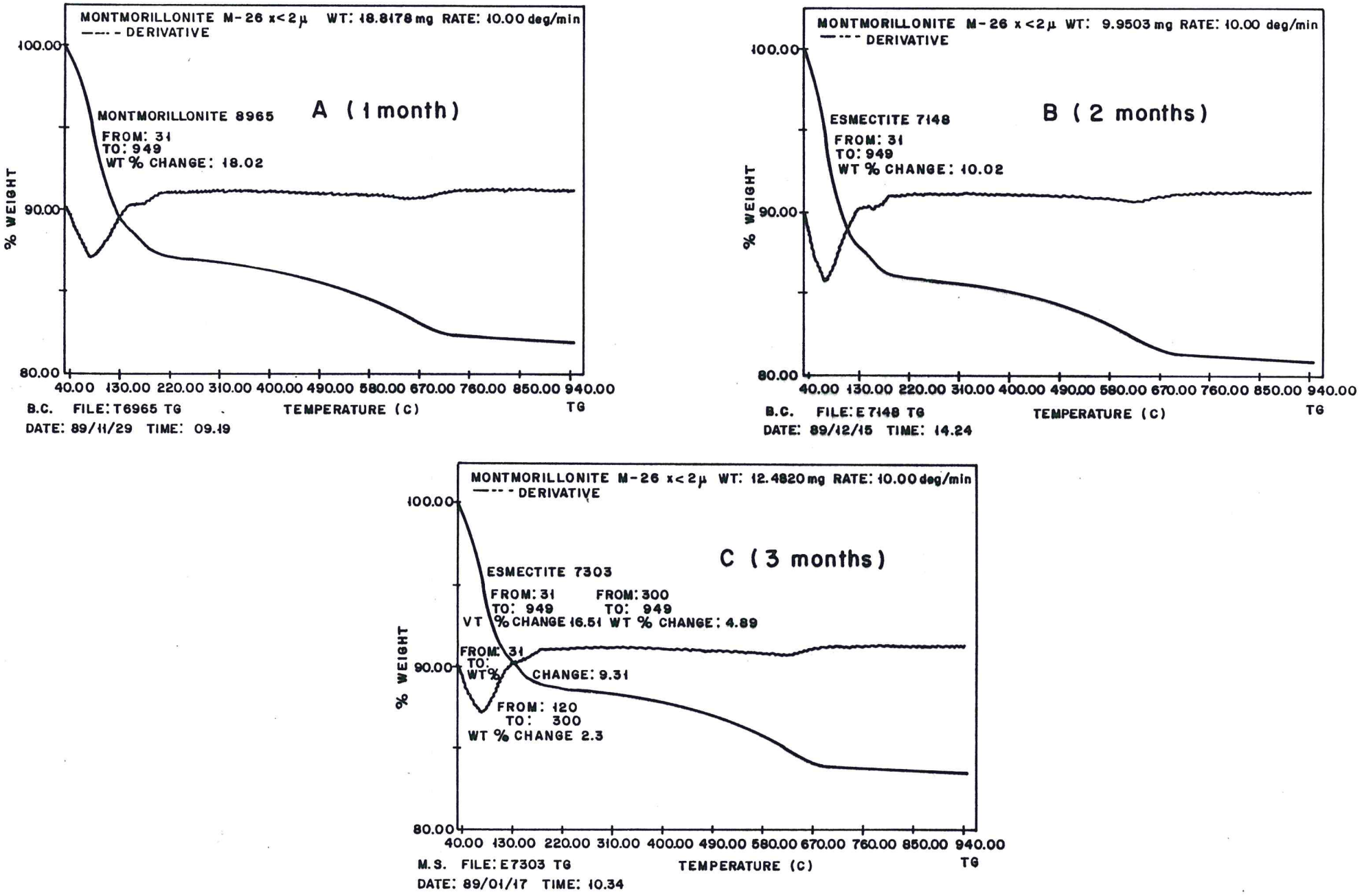

FIG. 52. TG curves of the x < 2μm fraction of sample M-26, treated with KCl 0.1 M at 175°C during 1, 2, 3 months.

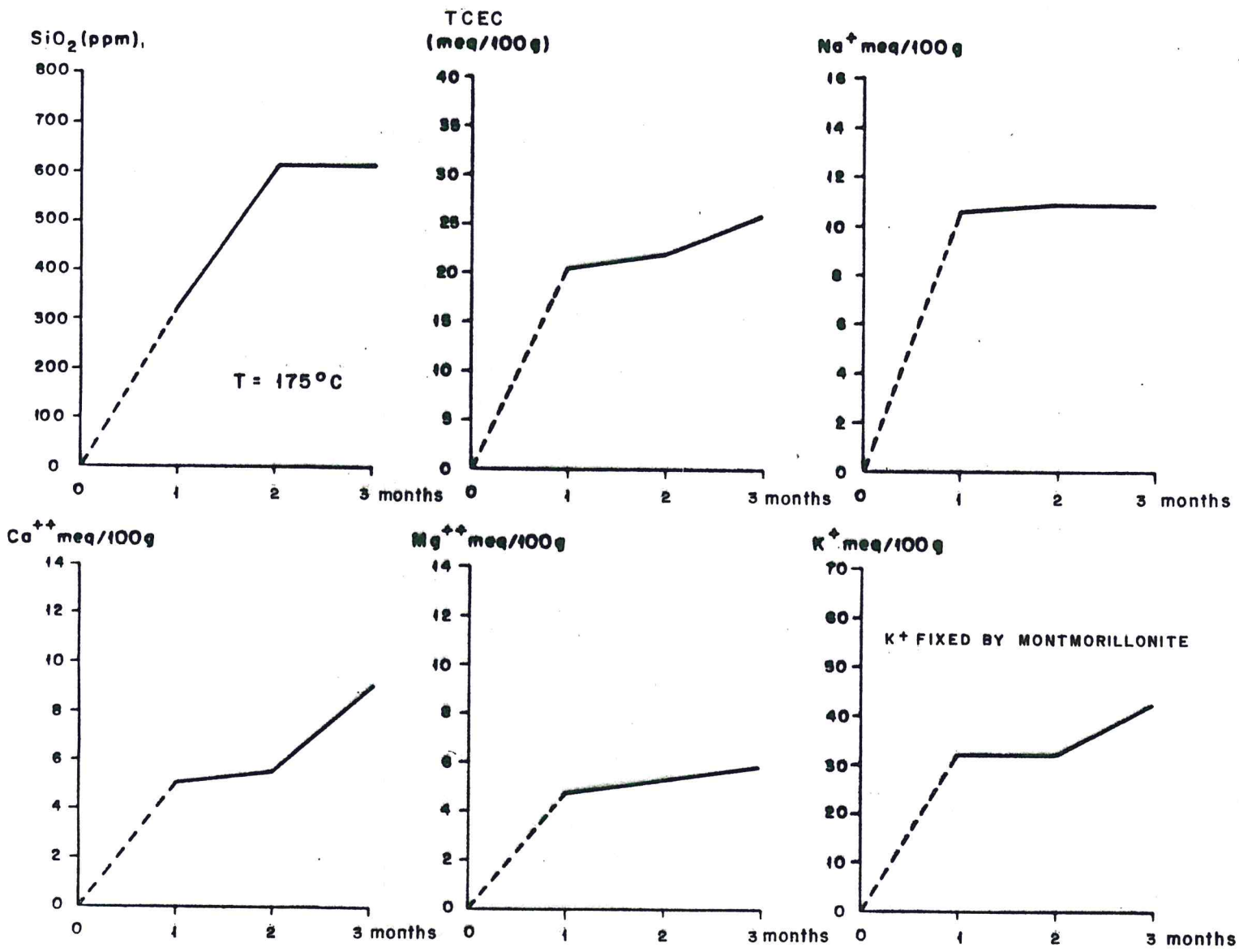

FIG. 53. Variation of SiO_2, CCC_T, Na^+, Ca^{++}, Mg^{++} and fixed K^+ as a function of the time of reaction.

9. CONCLUSIONS.

Based on the mechanical properties of the compacted blocks manufactured with montmorillonite (M-26), illite (M-15) and granite in different amounts and densities, the following can be deduced:

- The use of illitic clay as a basic material for the engineering barriers is doubtful, due to its mechanical and hydraulic properties, and it would be restricted to a clay content of 100% and final densities $\geq$ 1.8 g/cm^3. The addition of granite negatively influences the above mentioned properties.

- The resistance properties of the montmorillonitic blocks improve if approximately 25% of granite is added, and the swelling capacity is kept high (>10MPa); even for granitic amounts around 50%,if the dry density is higher than 1.9 g/cm^3, however, due to the "in situ" expected density decrease, it would be necessary to reduce the granite proportion below 25%. The hydraulic conductivity remains in acceptable values ($<10^{-12}$ m/s) for the 25% of granite in the mixture with montmorillonite.

- In the montmorillonite the resistance to compression and the sweeling properties reach eminently good values for initial values of moisture close to 20% in weight. In the case of illite the best moisture value is of the order of 5%.

- The process of consolidation with time, as a function of the loads supported by the clay barrier will favour the reduction of the pore index and the recovery of hydraulic conductivity values in the range of 10^{-14} m/s.

- The mobility in the barrier, due to diffussion processes, for ^{60}Co is slightly higher than for ^{137}Cs. The Da is in the

range of 10^{-13} m^2/s for both radionuclides. The addition of granite, up to 75%, slightly increases the apparent diffussion coefficient but without changing the order of manitude of those parameters.

- The montmorillonite has remained mineralogically stable for the time and essay condition used. It has not been detected a transformation to illite, and the only process originated has been one of partial cationic exchange in which K^+ has totally replaced the Na^+ and has replaced the available Ca^{++} and Mg^{++} in proportions lower than 31%.

10. REFERENCES.

ATABEK, R.; DARDAINE, M.; LAJUDIE, A.; PROUSE, P.; y BEZIAT, A.; Contrat CCE Nº FI 1W/0031, rapport d'avancement: janvier-juillet. 1987.

ATABEK, R.; LAJUDIE, A.; DARDAINE, M.; BEZIAT, A.; LECHELLE, J; PROUST, P.: Nearfield behaviour of clay barriers and their interaction with concrete. Contract CCE nº FI 1W/0031. Annual Progress Report. 1987.

BARAHONA, E.: Arcillas de ladrillería de la provincia de Granada. Evolución de algunos ensayos de materias primas. Tesis Doctoral. Universidad de Granada. 1974.

BISCAYE,P.E.; Mineralogy and sedimentation of recent deep-sea clays in the Atlantic Ocean and adjacent seas and oceans. Geol. Soc. Am. Bull. 76,803-832. 1965.

BOLT, G.H.; BRUGGENWERT, M.G.M.: Soil Chemistry. A. Basic Elements. Elsevier Scientific Publishing Company. New York. 1978.

BOWLES, J.E.; Propiedades geofísicas de los suelos. McGraw Hill. 1982.

DERLICH, S.; PARK, S.H.; BOISSON, J.Y.: Colmatage de fissures et de forages en formations géologiques fracturées (granites). Contract nº FI 1W/0058 F (CD). Decembre 1987.

LAJUDIE, A.; DARDAINE, M.; ATABEK, R.: Nearfield behaviour of clay barriers and their interaction with concrete. Contract CCE nº FI 1W/0031. Annual Progress Report. 1986.

MACKENZIE, R.C.; Differential Thermal Analysis Vol.1. Fundamental Aspects. Acad. Press. London & New York 775 pp. 1970.

MEGIAS, A.G.; ORDÓÑEZ, S.; CALVO, J.P.: Nuevas aportaciones al conocimiento geológico de la Cuenca de Madrid. **Rev. Mat. Proc. Geol.** 1983.

NOWAK, E.J.: The diffussion of Cs(I) and Sr(II) in liquid - saturated beds of backfill materials. Sandia Report SAND82-0750. Chemical Technology Division. Sandia National Laboratory. New Mexico. 1983.

PUSCH, R.; BÖRGERSON, L.; ERLSTRÖN, M.: Alteration of isolating properties of dense smectite clay in repository environment as examplified by seven pre-quaternary clays. SKB. Technical Report. December 1987.

REYES, E.; CABALLERO, E.; HUERTAS, F.; LINARES, J.; YUSTA, A.: Las bentonitas de la zona sur de Cabo de Gata (Almería). Geoquímica y Mineralogía. Acta Geológica Hispánica. V. 20 nº 314. 1985.

SCHULTZ, L.G.;Lithium and potassium absorption, deshidroxilation, temperature and structural water content of aluminous smectites. Clays and Clay Miner. 17,115-149. 1969.

SCHULTZ, L.G.; Mixed-layer clay in the Pierre Shale and equivalent rocks. Northern Great Plains region. U.S.Geol. Survey. Prof. Paper 1064-A. 1978.

SCHULTZ, L.G.: Quantitative interpretation of mineralogical composition from X-Ray and chemical data for the Pierre Shale. Geological Survey of USA. Professional Paper. 591-C, pp. C1-C31.

TARDY, V.: DUPLAY, J. FRITZ, B.: Stability fields of smectites and illites as a function of temperature and chemical composition. SKB. Technical Report. April 1987.

TORSTENFELT, B.: Migration of the Fission Products Strontium, Technetium, Iodine and Cesium in Clay. **Radiochimica Acta** 39. pp. 97-104. Munich. 1986.

TORSTENFELT, B.: Migration of the Actinides Thorium, Protactinium, Uranium, Neptunium, Plutonium and Americium in Clay. **Radiochimica Acta** 39. pp. 105-112. Munich. 1986.

WOOD, M.I.; ADEN, G.D.; LANE, D.L.; Evaluation of sodium bentonite and crushed basalt as waste package backfill materials. RHO-BW-ST-21P. October 1982.